Synbindin, A Novel Syndecan-2–binding Protein in Neuronal Dendritic Spines

Iryna M. Ethell, Kazuki Hagihara, Yoshiaki Miura, Fumitoshi Irie, and Yu Yamaguchi

The Burnham Institute, La Jolla, California 92037

Abstract. Dendritic spines are small protrusions on the surface of dendrites that receive the vast majority of excitatory synapses. We previously showed that the cell-surface heparan sulfate proteoglycan syndecan-2 induces spine formation upon transfection into hippocampal neurons. This effect requires the COOH-terminal EFYA sequence of syndecan-2, suggesting that cytoplasmic molecules interacting with this sequence play a critical role in spine morphogenesis. Here, we report a novel protein that binds to the EFYA motif of syndecan-2. This protein, named synbindin, is expressed by neurons in a pattern similar to that of syndecan-2, and colocalizes with syndecan-2 in the spines of cultured hippocampal neurons. In transfected hippocampal neurons, synbindin undergoes syndecan-2–dependent clustering. Synbindin is structurally related to yeast proteins known to be involved in vesicle transport. Immunoelectron microscopy localized synbindin on postsynaptic membranes and intracellular vesicles within dendrites, suggesting a role in postsynaptic membrane trafficking. Synbindin coimmunoprecipitates with syndecan-2 from synaptic membrane fractions. Our results show that synbindin is a physiological syndecan-2 ligand on dendritic spines. We suggest that syndecan-2 induces spine formation by recruiting intracellular vesicles toward postsynaptic sites through the interaction with synbindin.

Key words: heparan sulfate proteoglycan • dendritic spines • spine apparatus • synapse • vesicle transport

Introduction

The functioning of the nervous system depends upon an immensely complex and precise network of neurons. Cell adhesion is thought to play a critical role in the formation and maintenance of synaptic contacts between neurons (Hall and Sanes, 1993; Rose, 1995; Murase and Schuman, 1999; Serafini, 1999; Shapiro and Colman, 1999). Among different classes of molecules involved in cell adhesion, there is evidence that heparan sulfate proteoglycans (HSPGs)[1] are present in central synapses and neuromuscular junctions (Bondareff, 1967; Tani and Ametani, 1971; Eldridge et al., 1986; Cole and Halfter, 1996; Meier et al., 1998). Furthermore, HSPGs are suggested to play a role in regulating synaptic strength, thereby acting as key molecules for synaptic stabilization that underlie neural plasticity (Schubert, 1991). Based on these premises, we previously examined the expression of HSPGs in cultured rat hippocampal neurons. We demonstrated that syndecan-2, a member of the syndecan family of HSPGs, is concentrated in dendritic spines. Dendritic spines are numerous small membrane appendages protruding from dendritic surfaces that consist of specialized postsynaptic structures for the vast majority of excitatory synapses (Harris and Kater, 1994). Moreover, we showed that forced expression of syndecan-2 cDNA in young (1 wk in vitro) hippocampal neurons induces the formation of morphologically mature dendritic spines, which are normally seen after 3 wk in vitro (Ethell and Yamaguchi, 1999).

Syndecans are a major class of membrane-spanning HSPGs (Bernfield et al., 1992). There is increasing evidence that syndecans play significant roles in the organization of specific cell-surface structures, such as focal adhesions, through their interactions with cytoskeletal and signaling molecules (Carey et al., 1994; Woods and Couchman, 1994; Carey, 1997), and thereby provide an important linkage between extracellular event and intracellular signaling. The cytoplasmic domains of syndecans have structural features that strongly suggest their involvement in intracellular signaling and cytoskeletal interactions. These domains consist of a 13-residue juxtamembrane segment highly conserved among the members (C1 region), a variable segment, and another highly conserved 7–9-resi-

Address correspondence to Yu Yamaguchi, The Burnham Institute, 10901 North Torrey Pines Road, La Jolla, CA 92037. Tel.: (858) 646-3124. Fax: (858) 646-3199. E-mail: yyamaguchi@burnham.org

[1]*Abbreviations used in this paper:* CNS, central nervous system; DIV, days in vitro; E, embryonic day; GFP, green fluorescent protein; GRIP, glutamate receptor–interacting protein; GST, glutathione-S-transferase; His, hexahistidine; HSPG, heparan sulfate proteoglycan; PSD, postsynaptic density; RT, reverse transcriptase; RyR-2, ryanodine receptor; SNARE, soluble NSF attachment protein receptor; TRAPP, transport protein particle.

due segment (C2 region) at the COOH terminus of the molecule (Rapraeger and Ott, 1998). Most importantly, the Glu-Phe-Tyr-Ala (EFYA) sequence located at the COOH terminus is identical in all syndecans. Moreover, our previous studies have shown that a syndecan-2 mutant in which the EFYA sequence was deleted lacks the ability to induce the formation of dendritic spines, suggesting that the molecular interactions involving this motif are crucial for this phenomenon (Ethell and Yamaguchi, 1999).

It has been shown that syndecans interact with two PDZ domain–containing proteins, syntenin (Grootjans et al., 1997) and CASK/LIN2A (Cohen et al., 1998; Hsueh et al., 1998), through the EFYA motif. We previously proposed a model in which these PDZ domain–containing molecules are potential downstream effectors of syndecan-2 in dendritic spines (Ethell and Yamaguchi, 1999). In this model, we suggested that the spine formation is mediated by the cytoskeletal reorganization initiated by the syndecan-2–dependent clustering of PDZ domain proteins. In this paper, we report a novel syndecan-binding protein, synbindin. Unexpectedly, the structural property and the localization of synbindin suggest an entirely different mechanism for syndecan-2–induced spine formation.

Synbindin is a neuronal cytoplasmic protein identified by yeast two-hybrid screening using the syndecan-2 cytoplasmic domain as a bait. Although it bears homologies with several PDZ domain proteins and binds to the COOH-terminal EFYA tail of syndecan-2 (as do CASK and syntenin), synbindin does not contain any classical PDZ domains. Rather, synbindin shares homologies with yeast proteins involved in membrane trafficking and vesicle transport acting upstream of the soluble NSF attachment protein receptor (SNARE) complex. There is increasing evidence that functional postsynaptic maturation involves the regulation of vesicle trafficking in postsynaptic sites (Lledo et al., 1998; Turner et al., 1999). Dendritic spines contain intracellular membrane-bound cisterns, known as spine apparatus (Villa et al., 1992), which are frequently seen in the vicinity of the postsynaptic density (Harris and Stevens, 1988; Spacek and Harris, 1997). Synbindin is identified in vesicles in dendritic spines as well as in synapses. Furthermore, synbindin forms clusters in dendritic spines when syndecan-2 is coexpressed in neurons. Our observations suggest a role for cell-surface syndecan-2 in the translocation of postsynaptic vesicular compartments through the cytoplasmic interaction with this novel syndecan-2–binding molecule.

Materials and Methods

Yeast Two-Hybrid Assays

Yeast two-hybrid screens were performed using the L40 yeast strain, where the expression of both the reporter genes HIS3 and LacZ are driven by minimal GAL1 promoters fused to LexA-binding sites. A bait consisting of the entire cytoplasmic domain of the syndecan-2 fused in-frame to the LexA DNA–binding domain was constructed by PCR with the BTM116 vector. An embryonic mouse cDNA library constructed into the NotI site of pVP16 containing the Leu2 activation domain (Vojtek and Hollenberg, 1995; a gift from Dr. Erkki Ruoslahti, The Burnham Institute) was screened with the syndecan-2 bait. Positive clones were selected by His prototrophy and assayed for β-galactosidase activity. Double-positive clones were isolated and characterized by sequencing. A double-positive clone (clone 28), which encodes a putative cytoplasmic protein with similarities to several PDZ domain–containing proteins (see Results), was further investigated as described in this paper. We named this protein synbindin. The specificity of the interaction between synbindin and the cytoplasmic domain of syndecan-2 was analyzed by two-hybrid assays (see Fig. 1 A). For this, we generated (by PCR) the following additional baits of the syndecan cytoplasmic domains: (1) a syndecan-2 deletion mutant lacking the COOH-terminal EFYA sequence (syndecan-2ΔEFYA); (2) a syndecan-4 deletion mutant lacking the COOH-terminal EFYA sequence (syndecan-4ΔEFYA); and (3) a bait with reverse sequence of syndecan-2 cytoplasmic domain. To determine the syndecan-2–binding site in synbindin, we generated by PCR four Leu2 fusion constructs representing the NH_2-terminal half of synbindin (N-Sbd), the PDZ-related domain (P-Sbd), the COOH-terminal half (C-Sbd), and the PDZ-related domain plus the COOH-terminal half (P/C-Sbd) (see Fig. 2 D). Two-hybrid assays were performed as described above using HIS3 and LacZ as reporter genes.

Cloning of the Full-length Synbindin cDNA

The full-length synbindin cDNA was isolated from a mouse brain λZAP cDNA library (Stratagene) with clone 28 as a probe. Four cDNA clones were isolated. One of the isolated clones contained an entire open reading frame encoding 219 amino acid residues. Full-length sequence of mouse synbindin cDNA was determined from this clone. Human and *Caenorhabditis elegans* synbindin homologues were identified in EST database by a BLAST search, and their entire sequences were reconstituted from overlapping EST clones.

Production of Glutathione-S-Transferase (GST) Fusion Proteins

A 663-bp EcoRI-XhoI fragment containing the entire coding region of mouse synbindin was amplified by PCR with the following primers and ligated into pGEX-4T-1 (Amersham Pharmacia Biotech): 5′ primer, ACCCGGAATTCATGGCGATTTTTACCGTGTAC; and 3′ primer, CGGCCGCTCGAGCTATGACCCAGGTCCAAAAGT. The GST-synbindin expression plasmid as well as insertless pGEX-4T-1 were transfected into BL21 *Escherichia coli* strains according to the manufacturer's instructions. BL21 cells were lysed by sonication in 20 mM Tris-HCl containing 0.15 M NaCl, 1 mM EDTA, 1 mM PMSF, 10 μg/ml pepstatin, 10 μg/ml aprotinin, and 2 μg/ml leupeptin. Sarkosyl was added to lysates to a final concentration of 1.5%, and the lysates were gently mixed for 15 min. After centrifugation, supernatants were adjusted to 2% Triton X-100 and 1 mM $CaCl_2$, and GST-synbindin was purified with glutathione-agarose.

Antibodies

Two polyclonal antibodies against mouse synbindin were generated for this study. Rabbit anti-synbindin peptide antibody was raised against a synthetic peptide acetyl-CELFDQNLKLALELAEKV-amide (corresponding to amino acids 195–213 of mouse synbindin) and affinity-purified on amino-link/agarose beads coupled with the synthetic peptide (Quality Controlled Biochemicals). The other polyclonal antibody (No. 157) was raised against the bacterially produced recombinant synbindin protein released from GST-synbindin fusion protein by proteolytic cleavage and affinity-purified using synbindin-GST fusion protein coupled to glutathione-agarose. Other antibodies used in this study were as follows: anti–c-Myc rabbit polyclonal antibody A14 (Santa Cruz Biotechnology, Inc.); anti–syndecan-2 mAb 6G12 (Lories et al., 1989; a gift from Dr. Guido David, University of Leuven, Leuven, Belgium); anti–syndecan-2 polyclonal antibody (Kim et al., 1994; a gift from Dr. Merton Bernfield, Harvard Medical School, Boston, MA); anti–PSD-95 mAb 6G6 (Affinity Bioreagents, Inc.); antisynaptophysin and anti-MAP2 mAbs (Sigma Chemical Co.); and anti-CASK polyclonal antibody (Hsueh et al., 1998; a gift from Dr. Morgan Sheng, Howard Hughes Medical Institute, Harvard Medical School, Boston, MA).

Transfection of 293 Cells, GST Pull-down, and Coimmunoprecipitation Experiments

Human 293 cells were grown in DME supplemented with 10% FCS and antibiotics. Approximately 70% confluent 293 cells in 10-cm dishes were transfected with 20 μg of an expression vector for Myc-tagged full-length syndecan-2 (a gift from Dr. Morgan Sheng; Hsueh et al., 1998) or a control vector using the calcium phosphate method (Ethell and Yamaguchi, 1999). 1 d after transfection, transfected cells were treated with or without

heparitinase (Seikagaku America), and then sonicated in 25 mM Tris-HCl, pH 8.0, containing 0.15 M NaCl, 1% Triton X-100, 5 mM EDTA, 1 mM PMSF, 5 mM DTT, 10 μg/ml pepstatin, 10 μg/ml aprotinin, and 2 μg/ml leupeptin (lysis buffer). Heparitinase treatment was performed in 20 mM Hepes, pH 7.0, containing 0.15 M NaCl and 1 mM calcium acetate for 1 h at 37°C. After sonication, cell lysates were cleared by centrifugation at 14,000 rpm in a microcentrifuge. For pull-down assays, cleared lysates were incubated with glutathione-agarose beads charged with unfused GST or GST-synbindin fusion protein for 1 h at 4°C. After incubation, beads were washed once with lysis buffer and five times with 25 mM Tris-HCl, pH 7.4, containing 0.5 M NaCl and 0.2% Triton X-100 at room temperature. The materials retained on the beads were eluted with SDS-PAGE sample buffer and detected by SDS-PAGE and immunoblotting as described previously (Belliveau et al., 1997). The Myc-tagged syndecan-2 pulled down by GST-synbindin was detected with either anti–syndecan-2 mAb (clone 6G12; a gift from Dr. Guido David; 1:1,000 dilution) or anti-Myc polyclonal antibody (A14; Santa Cruz Biotechnology; 1:1,000 dilution).

For coimmunoprecipitation assays, we generated intact and ΔEFYA syndecan-2 cDNAs that are epitope-tagged with the FLAG sequence (designated as FLAG-syndecan-2 and FLAG-syndecan-2ΔEFYA, respectively). A FLAG tag (DYKDDDDK) was inserted at the unique SpeI site in the ectodomain of syndecan-2. These FLAG-tagged syndecan-2 constructs were transfected into 293 cells with or without cotransfection of a synbindin expression construct in which the c-Myc epitope was added to the NH_2 terminus of synbindin (Myc-synbindin). Cell lysates from these transfectants were prepared as described above without heparitinase treatment. The lysates were incubated with the A14 anti-Myc polyclonal antibody for 2 h at 4°C, followed by an incubation with protein A–Sepharose for 1 h. Bound materials were eluted with SDS-PAGE sample buffer, separated on an 8–16% gel, and immunoblotted with the M2 anti-FLAG mAb (Sigma Chemical Co.; 1:1,000 dilution) to detect coprecipitated FLAG-tagged syndecan-2.

Production of Hexahistidine (His)-tagged Syndecan-2 Cytoplasmic Domains and Overlay Assays

For preparation of His-tagged syndecan-2 cytoplasmic domains, a DNA fragment encoding the entire syndecan-2 cytoplasmic domain was amplified by PCR and inserted into EcoRI-XhoI–linearized pET-30a (Novagen). The construct for His-tagged ΔEFYA syndecan-2 cytoplasmic domain was then generated by point mutagenesis of the AAG codon for the lysine residue preceding the EFYA sequence to a stop codon (TAG). These His-tagged cytoplasmic domains (intact and ΔEFYA) were expressed in BL21 (DE3) cells and purified on ProBond resin (Invitrogen). For overlay assays, equal amounts of the intact and ΔEFYA cytoplasmic domains were loaded on a 10–20% tricine gel and blotted onto a nitrocellulose membrane. The membrane was stained with Ponceau S to ascertain that equivalent amounts of the intact and ΔEFYA cytoplasmic domains were applied. The membrane was blocked with 5% nonfat dry milk in 25 mM Tris-HCl, pH 7.4, containing 0.15 M NaCl and 0.3% Tween 20 (TBS-Tween) overnight at 4°C, and incubated with 50 μg/ml of purified GST-synbindin in TBS-Tween containing 1 mM DTT and 2% BSA for 2 h at room temperature. Bound GST-synbindin was detected with goat anti-GST antibody (Amersham Pharmacia Biotech; 1:3,000 dilution) and HRP-conjugated anti-goat IgG (Sigma Chemical Co.; 1:5,000 dilution).

Primary Cultures and Transfection of Hippocampal Neurons

Cultures of rat hippocampal neurons were prepared as described previously from E17 embryos (Ethell and Yamaguchi, 1999). Transient transfection of hippocampal neurons was performed at 1 d in vitro by the calcium phosphate coprecipitation method (Ethell and Yamaguchi, 1999). For the analysis of coclustering of syndecan-2 and synbindin, hippocampal neurons were transfected with an expression vector containing synbindin-green fluorescent protein (GFP) fusion protein alone, or together with either the full-length syndecan-2 expression vector or the syndecan-2ΔEFYA expression vector (for detail of these vectors see Ethell and Yamaguchi, 1999). Cotransfection of the synbindin-GFP and the syndecan-2/syndecan-2ΔEFYA expression vectors were performed at the ratio of 1:10 (Ethell and Yamaguchi, 1999). We confirmed that, under this condition, essentially every GFP-positive cell coexpresses syndecan-2/syndecan-2ΔEFYA as demonstrated by immunostaining for syndecan-2. The frequency of synbindin clustering in these cotransfected cultures was determined as the percentage of cells that show >10 synbindin clusters in their dendrites to the total GFP-positive cells. A total of 40 neurons were scored in four sampling windows for each culture.

Immunofluorescence and Confocal Imaging

Hippocampal neurons transfected with synbindin-GFP alone or together with syndecan-2 were examined 8 d after transfection (9 DIV) by a confocal microscopy as previously described (Ethell and Yamaguchi, 1999). Synbindin localization was identified by GFP fluorescence. Transfected neurons were also immunostained with either anti–synapsin I polyclonal antibody (1:100 dilution; a gift from Dr. Andrew Czernik), anti–syndecan-2 polyclonal antibody (1:100 dilution; a gift from Dr. Merton Bernfield) or anti-MAP2 mAb (1:100 dilution; Sigma Chemical Co.). Rhodamine-conjugated anti-rabbit IgG (1:100 dilution; Chemicon International) or rhodamine-conjugated anti-mouse IgG (1: 50 dilution; Cappel Laboratories) were used as secondary antibodies.

To localize endogenous synbindin, hippocampal neurons at 1, 2, 3, and 4 wk in vitro were double-immunostained with affinity-purified antisynbindin polyclonal antibody (No. 157; 1:100 dilution) and antisynaptophysin mAb (1:100 dilution; Sigma Chemical Co.) or antisynbindin polyclonal antibody and anti-MAP2 mAb (1:100 dilution; Sigma Chemical Co.). FITC-conjugated anti-rabbit IgG (1:100 dilution; Chemicon International) and rhodamine-conjugated anti-mouse IgG (1:50 dilution; Cappel Laboratories) were used as secondary antibodies. After staining, cells were mounted with fluorescence H-1000 medium (Vector Laboratories) and analyzed on a confocal laser scanning microscope (model MRC1024; Bio-Rad Laboratories).

RNA Purification, Reverse Transcriptase (RT)-PCR, and Northern Blot Analysis

Total RNA was extracted from cultures of rat hippocampal neurons at different time points by using Trizol reagents (Life Technologies, Inc.). RT-PCR was performed with 2 μg of the total RNA with the following primer pair: 5′ primer, GAGGCTGAGAAGACTTTCAG; 3′ primer, AACATCGAGGCCAGCATAAG (corresponding to nucleotide numbers 291–311 and 537–557 of mouse synbindin, respectively). PCR products were analyzed on an agarose gel. The identity of amplified bands as synbindin was confirmed by sequencing. For Northern analysis, a mouse multiple tissue Northern blot (CLONTECH Laboratories, Inc.) was hybridized with a ^{32}P-labeled RNA probe of mouse synbindin, which was synthesized with T3 RNA polymerase (Promega) using pBluescript II SK+ containing mouse synbindin cDNA as a template. Hybridization was performed according to the manufacturer's instructions.

In Situ Hybridization

Adult C57BL/6 mice were anesthetized and perfused transcardially with 4% paraformaldehyde in PBS. Whole brains were dissected, immersed in 30% sucrose in PBS overnight at 4°C, and embedded in OCT compound (Miles). Cryostat sections (20-μm thick) were hybridized with digoxigenin-labeled RNA probes as described previously (Watanabe et al., 1995). Antisense and sense RNA probes for mouse synbindin and syndecan-2 were in vitro transcribed from pBluescript II SK+ containing full-length synbindin or syndecan-2 cDNA using either T3 or T7 RNA polymerase (Promega) and the digoxigenin RNA labeling kit (Boehringer Mannheim).

Subcellular Fractionation and Coimmunoprecipitation of Endogenous Proteins

Subcellular fractions of adult mouse cortex or hippocampus were prepared as described by Li et al. (1996) and Torres et al. (1998). In brief, adult mouse cortex was homogenized in 4 mM Hepes, pH 7.4, containing 0.32 M sucrose, 1 mM PMSF, 10 μg/ml pepstatin, 10 μg/ml aprotinin, and 2 μg/ml leupeptin with a Teflon head tissue grinder. Homogenates were centrifuged at 1,000 *g* for 10 min. The supernatant was collected and centrifuged at 12,000 *g* for 15 min, yielding a pellet (P2) and supernatant (S2). Supernatant (S2) was further centrifuged at 100,000 *g* for 90 min. The resulting supernatant represents the soluble fraction. The P2 pellet was resuspended in homogenization buffer and represented crude synaptosomes fraction. The crude synaptosome fraction was lysed by osmotic shock by adding 10 vol of ice-cold water containing protease inhibitors and homogenized. The synaptic membrane fraction was pelletted from this homoge-

nate by centrifugation at 33,000 *g* for 20 min, and the supernatant contained synaptic vesicles. Equal amounts of proteins (50 μg per lane) from each fraction were resolved by SDS-PAGE on an 8–16% gradient gel, transferred to a nitrocellulose membrane, and analyzed by immunoblotting. The subcellular fractions were examined by immunoblotting with anti–PSD-95 (a marker for postsynaptic density), antisynaptophysin (a marker for synaptic vesicles), and anti-CASK antibodies. To identify subcellular localization of synbindin, the subcellular fractions were probed with antisynbindin peptide antibody at 1:500 dilution. As a control for specificity of antisynbindin antibody, blots were reprobed with preimmune serum.

For coimmunoprecipitation of synbindin and syndecan-2 from the brain, the synaptic membrane fraction was solubilized with 1% CHAPS in TBS containing a protease inhibitor cocktail (Sigma Chemical Co.). After removing insoluble materials by centrifugation, supernatants were incubated with protein G–Sepharose charged with anti–syndecan-2 mAb (6G12) or uncharged protein G–Sepharose at 4°C for 2 h. Bound materials were eluted with SDS-PAGE sample buffer, separated on a 8–16% gel, and immunoblotted with antisynbindin polyclonal antibody (No. 157).

Immunohistochemistry and Immunoelectron Microscopy

Immunohistochemistry of synbindin was performed with free-floating sections. In brief, adult mice were perfused transcardially with ice-cold 0.9% saline followed by fixation in 4% paraformaldehyde. Free-floating Vibratome sections (50–100-mm thick) of the whole brain were first washed in 0.1 M Tris-HCl, pH 7.6, incubated with 1% hydrogen peroxide for 30 min, and washed again with 50 mM Tris-HCl, pH 7.6, containing 0.15 M NaCl (TBS). Sections were blocked for 30 min with TBS containing 0.1% Triton X-100, 3% normal goat serum and 0.1% BSA (blocking buffer), and then with the avidin-biotin blocking kit (Vector Laboratories). Blocked sections were incubated with affinity-purified antisynbindin antibody (No. 157), which was diluted in the blocking buffer at 2 μg/ml at room temperature overnight. After washing with TBS containing 0.1% Triton X-100 (TBS-T), sections were incubated with biotinylated goat anti–rabbit antibody (Vector Laboratories) at a dilution of 1:200 for 2 h, washed with TBS-T, and incubated with avidin-biotin HRP complex (Vectastain Elite; Vector Laboratories) for 2 h at room temperature. After washing with TBS-T and with 50 mM Tris-HCl, pH 7.6, sections were reacted with 0.05% diaminobenzidine and 0.001% hydrogen peroxide in TBS.

For electron microscopy, adult mice were perfused through the aorta with ice-cold 0.9% NaCl and then with 4% glutaraldehyde and 0.1% paraformaldehyde in 0.1 M phosphate buffer, pH 7.4. The brain was dissected and postfixed in the same fixative for 1 h at room temperature, and coronal sections (100 μm) of the cerebral cortex were cut by Vibratome. Preembedding immunostaining was performed as follows: the sections were cut into small pieces and incubated in PBS containing 50 mM glycine for 5 min, washed three times with PBS, and blocked with PBS containing 20% normal goat serum and 0.05% Triton X-100 for 1 h. Blocked sections were incubated with affinity-purified antisynbindin antibody (No. 157) or normal rabbit IgG (as a negative control) diluted in PBS containing 3% normal goat serum, 0.05% Triton X-100 (PBS-T) overnight. The next day, sections were washed three times with PBS-T and incubated with anti-rabbit nanogold conjugates (1.4 nm; Nanoprobes Inc.) at a dilution of 1:100 in PBS-T for 90 min at room temperature. After four washes with PBS-T, the sections were further washed four times with deionized water and treated for 7 min with gold enhancer-EM formulation (Nanoprobes Inc.) to enhance immunoreactive signals. The sections were postfixed in 1% osmium in PBS for 30 min, washed with PBS, dehydrated through graded ethanol solutions, and infiltrated with propylene oxide to Epon resin (Ted Pella). The sections were sandwiched between strips of ACLAR plastic film (Ted Pella), flattened between glass sheets, and polymerized in Epon Araldite at 60°C for 24 h. Epon-embedded samples were glued onto resin blocks, and ultrathin sections were cut and collected on 200-mesh collodion-coated copper grids (Electron Microscopy Sciences). The grids were poststained with uranyl acetate and lead citrate, and examined on a Hitachi 600E transmission electron microscope. The distribution of gold particles was analyzed by counting particles using NIH Image software as described in Srivastava et al. (1998).

Results

Identification and Cloning of a Novel Syndecan-2–binding Protein, Synbindin

To identify novel syndecan-2–binding proteins, we performed a yeast two-hybrid screen using the syndecan-2 cytoplasmic domain as bait. Screening of a mouse embryo library resulted in isolation of positive colonies selected by HIS prototrophy and β-galactosidase activity. One of the isolates (clone 28) showed a strictly specific interaction pattern with a series of control baits. The specificity of the interaction between clone 28 and the syndecan cytoplasmic domain was studied further by two-hybrid assays (Fig. 1, A and B). This study demonstrated that clone 28 recognizes the COOH-terminal EFYA sequence of syndecans. As shown in Fig. 1, clone 28 binds not only the syndecan-2 domain, but also the syndecan-4 cytoplasmic domain, suggesting that it recognizes a region conserved in both syndecans. Because syndecan-2 and syndecan-4 share the COOH-terminal EFYA motif, we deleted this motif from baits (designated as syndecan-2ΔEFYA and syndecan-4ΔEFYA, respectively). Both syndecan-2ΔEFYA and syndecan-4ΔEFYA mutants failed to bind clone 28 (Fig. 1 B). These results indicate that it binds to the COOH terminus of syndecans, as do syntenin and CASK.

A full-length cDNA for this gene was isolated from a mouse brain library. The entire open reading frame encodes a protein consisting of 219 amino acid residues with a predicted molecular mass of ~24 kD (Fig. 1 C). The clones isolated by two-hybrid screening corresponded to amino acid residues 18–182 of this protein. No signal sequence or transmembrane domain was identified in the protein. We named this protein synbindin. Synbindin has 48% amino acid identity with the *C. elegans* F36D4.2 gene (U53181) and 29% identity with a 23-kD yeast protein, tentatively called p23 (Sacher et al., 1998; Fig. 1, C and D). These *C. elegans* and yeast proteins are likely to be orthologues to mouse synbindin, suggesting that synbindin is highly conserved across species. While no functional data are available for the *C. elegans* gene, the yeast p23 is a component of a multiprotein complex (transport protein particle [TRAPP]) involved in vesicle docking and fusion (Sacher et al., 1998). This suggests that synbindin may be involved in vesicular transport in mammalian cells.

A homology search further identified three segments of substantial homology with proteins known to be involved in vesicular transport as well as synaptic functions (Fig. 1, F). First, an ~60-amino acid residue segment in the NH_2-terminal part of synbindin bears homologies with several PDZ domains. Weak but significant homologies (20–30% identity; 40–50% similarity) were identified with the following: the sixth PDZ domain of glutamate receptor–interacting protein (GRIP) 1 and GRIP2 (Dong et al., 1997; Srivastava et al., 1998; Wyszynski et al., 1999); the seventh PDZ domain of the 5-HT_{2C} receptor–binding protein MUPP1 (Ullmer et al., 1998); the fourth PDZ domain of human INAD-like protein (Phillipp and Flockerzi, 1997); and the second PDZ domains of Mint-1, -2, and -3 (Duclos et al., 1993; Okamoto and Südhof, 1997; Takahashi and Tabira, 1999). All of these proteins have been implicated in synaptic functions. The homology with these PDZ domains

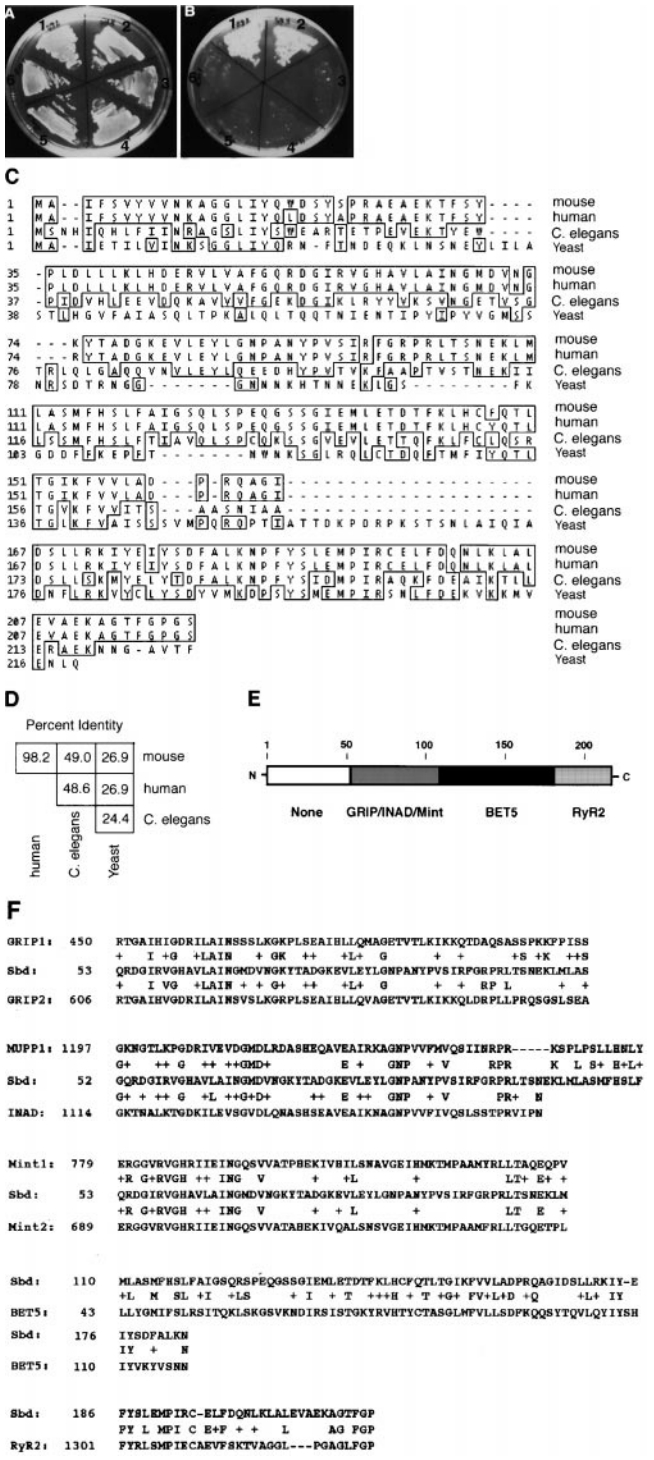

Figure 1. Synbindin is a novel protein that interacts with the EFYA motif of syndecans. (A and B) Binding of clone 28 (synbindin) to the syndecan cytoplasmic domains. Two-hybrid assays were performed with the Leu2 activation domain containing clone 28 and the LexA DNA–binding domain containing one of following syndecan cytoplasmic domains: syndecan-2 (1); syndecan-4 (2); a scrambled amino acid sequence of syndecan-2 (3); syndecan-4ΔEFYA (4); and syndecan-2ΔEFYA (5 and 6). Transformants were grown on a Leu^-/Trp^- plate (A) or a $His^-/Leu^-/Trp^-$ plate (B). (C) Amino acid sequences of mouse synbindin deduced from its full-length cDNA sequence in comparison with the putative human synbindin (AAF21897.1), *C. elegans* F36D4.2 (AAA93486), and the yeast p23 (Sacher et al., 1998). Identical amino acid residues are shown in a box. The nucleotide sequence data of mouse synbindin is available from GenBank/EMBL/DDBJ under accession number AF233340. (D) Percent amino acid identity between mouse synbindin and its human, nematode, and yeast homologues. (E) A model of the synbindin molecule. Each box represents a region that shows homology with the known protein(s) indicated below the box. Numbers indicate amino acid residues. (F) Alignment of mouse synbindin (*Sbd*) with human GRIP1 (AJ133439) and rat GRIP2 (AF112182), human MUPP1 (AF093419) and human INAD (AJ001306), rat Mint1 (AF029105) and human Mint2 (AF029108), yeast BET5 (NP_013634), and human RyR-2 (X98330).

does not encompass the entire PDZ domain, but is restricted to the COOH-terminal part of the domain. Therefore, this segment of synbindin does not constitute a classical PDZ domain. Second, a 76-amino acid residue segment in the middle of the molecule shows a strong similarity with the yeast gene BET5 (Fig. 1 F). BET5 is a gene involved in vesicle transport in yeast. A null mutation of BET5 blocks ER-to-Golgi transport (Jiang et al., 1998). Moreover, like p23, the protein product of BET5 (Bet5p) is a component of the yeast TRAPP complex (Jiang et al., 1998). Considering the phylogenetic distance between mouse and yeast, the homology between synbindin and BET5 in this segment is quite high (30% identity; 50% similarity). These observations further supports the notion that synbindin is involved in vesicular transport. Finally, the 35 residue COOH-terminal segment shows 45% identity (52% similarity) to a short cytoplasmic segment of the cardiac muscle ryanodine receptor (RyR-2), which is a calcium release channel on the membrane of intracellular Ca^{2+} stores (Tunwell et al., 1996). Taken together, synbindin consists of four regions: the NH_2-terminal region, which has no significant homology with any known proteins; a PDZ-related region; a BET5-related region; and a COOH-terminal tail similar to a short segment of RyR-2 (Fig. 1 E)

Characterization of the Synbindin–Syndecan-2 Interaction

To further assess the specificity of the synbindin–syndecan-2 interaction, we performed pull-down and coimmunoprecipitation assays. For pull-down assays, glutathione-agarose beads charged with synbindin-GST fusion protein or nonfused GST were incubated with lysates of 293 cells expressing Myc-tagged syndecan-2. Bound materials were probed by immunoblotting with anti–syndecan-2 mAb or anti-Myc polyclonal antibody (Fig. 2 A). (Note that, in 293 cells, most syndecan-2 molecules are expressed as a 34-kD simple glycoprotein lacking heparan sulfate chains [see Fig. 2, A, d].) As shown in Fig. 2, GST-synbindin brought down syndecan-2 from the cell lysates (Fig. 2 A, a and b). No syndecan-2 was brought down with nonfused GST (Fig. 2 A, c) or from control transfected 293 cells (Fig. 2 A, a and b, lane 1). To examine coimmunoprecipitation of synbindin and syndecan-2, 293 cells were cotransfected with FLAG-tagged syndecan-2 (either FLAG-syndecan-2 or FLAG-syndecan-2ΔEFYA) and Myc-tagged synbindin. The FLAG-syndecan-2 was precipitated from the lysate of cotransfected cells with anti-Myc antibody (Fig. 2 B, c,

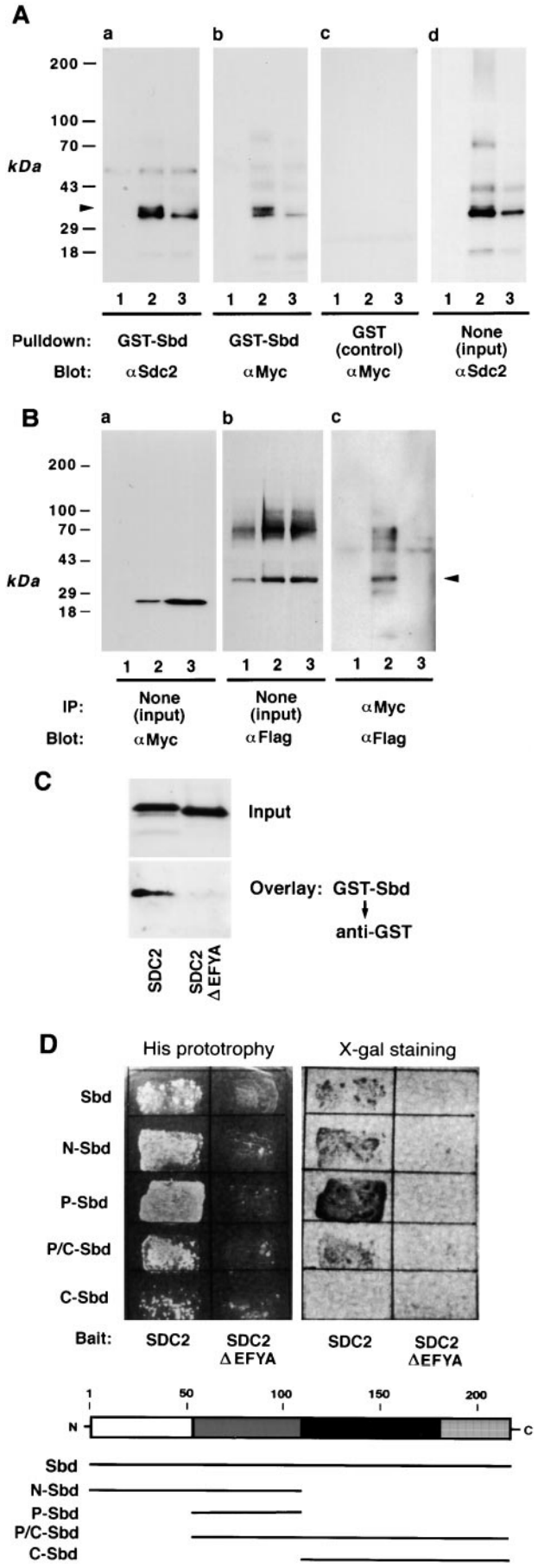

lane 2). No coimmunoprecipitation was observed when synbindin was not introduced into cells (Fig. 2 B, c, lane 1). The syndecan-2ΔEFYA mutant was not coprecipitated with synbindin (Fig. 2 B, c, lane 3).

Direct binding between synbindin and the syndecan-2 cytoplasmic domain was examined using purified His-tagged syndecan-2 cytoplasmic domains and GST-synbindin. GST-synbindin bound to His-tagged syndecan-2 cytoplasmic domain in the overlay assay (Fig. 2 C). Consistent with pull-down and coimmunoprecipitation assays, the ΔEFYA cytoplasmic domain failed to bind GST-synbindin.

Finally, we analyzed the region of synbindin that interacts with syndecan-2 by using two-hybrid assays. The full-length synbindin and four truncated forms were tested with baits of the intact and ΔEFYA syndecan-2 cytoplasmic domains (Fig. 2 D). The three fragments containing the PDZ-like segment showed a strong interaction with the intact syndecan-2 cytoplasmic domain. The strongest of the three was the P-Sbd fragment, which consists only of the PDZ-like segment followed by the N-Sbd and P/C synbindin fragments. The fragment without the PDZ-like segment (C-Sbd) did not display a signal above background. The ΔEFYA bait did not interact with any fragments. Taken together, these binding studies establish that syn-

Figure 2. Characterization of the synbindin–syndecan-2 interaction by pull-down, coimmunoprecipitation, ligand overlay, and two-hybrid assays. (A) GST pull-down assay. Lysates from human 293 cells transfected with Myc-tagged syndecan-2 were pulled down with GST-synbindin fusion protein (a and b) or non-fused GST (c) and immunoblotted with anti–syndecan-2 mAb 6G12 (a) or anti-Myc polyclonal antibody A14 (b and c). In d, cell lysates were directly immunoblotted with anti–syndecan-2 mAb without pull-down. In each panel, three different lysates were tested: (lane 1) lysates from 293 cells transfected with a control vector; (lane 2) lysates from 293 cells transfected with Myc-tagged syndecan-2, which were undigested; and (lane 3) lysates from 293 cells transfected with Myc-tagged syndecan-2, which were digested with heparitinase. The arrowhead indicates the 34-kD syndecan-2 core protein. (B) Coimmunoprecipitation of synbindin and syndecan-2. The 293 cells were transfected with FLAG-syndecan-2 alone (lane 1), FLAG-syndecan-2 and Myc-synbindin (lane 2), or the FLAG-syndecan-2ΔEFYA deletion mutant and Myc-synbindin (lane 3). The cell lysates were immunoprecipitated with anti-Myc polyclonal antibody and immunoblotted with anti-FLAG antibody (c). The arrowhead indicates the syndecan-2 core protein. Note that the intact syndecan-2 was coimmunoprecipitated with synbindin (c, lane 2), whereas the syndecan-2ΔEFYA deletion mutant was not (c, lane 3). In a and b, the lysates were directly immunoblotted with anti-Myc antibody (a) and anti-FLAG antibody (b), respectively, to show that similar amounts of proteins were expressed. (C) GST-synbindin overlay assay. His-tagged recombinant proteins of intact syndecan-2 cytoplasmic domain (*SDC2*) and ΔEFYA cytoplasmic domain (*SDC2ΔEFYA*, right lane) were resolved on a 10–20% tricine gel, blotted, and overlaid with GST-synbindin (bottom panel) as described in Materials and Methods. (top panel) Ponceau S staining of the blot. (D) Two-hybrid assays to analyze the syndecan-2–binding site in synbindin. Four synbindin fragments (shown in the bottom panel) were tested with two syndecan-2 baits: one representing the intact syndecan-2 cytoplasmic domain (*SDC2*) and the other representing the ΔEFYA cytoplasmic domain (*SDC2ΔEFYA*). The interactions were scored by His prototrophy (left) and β-galactosidase activity (right).

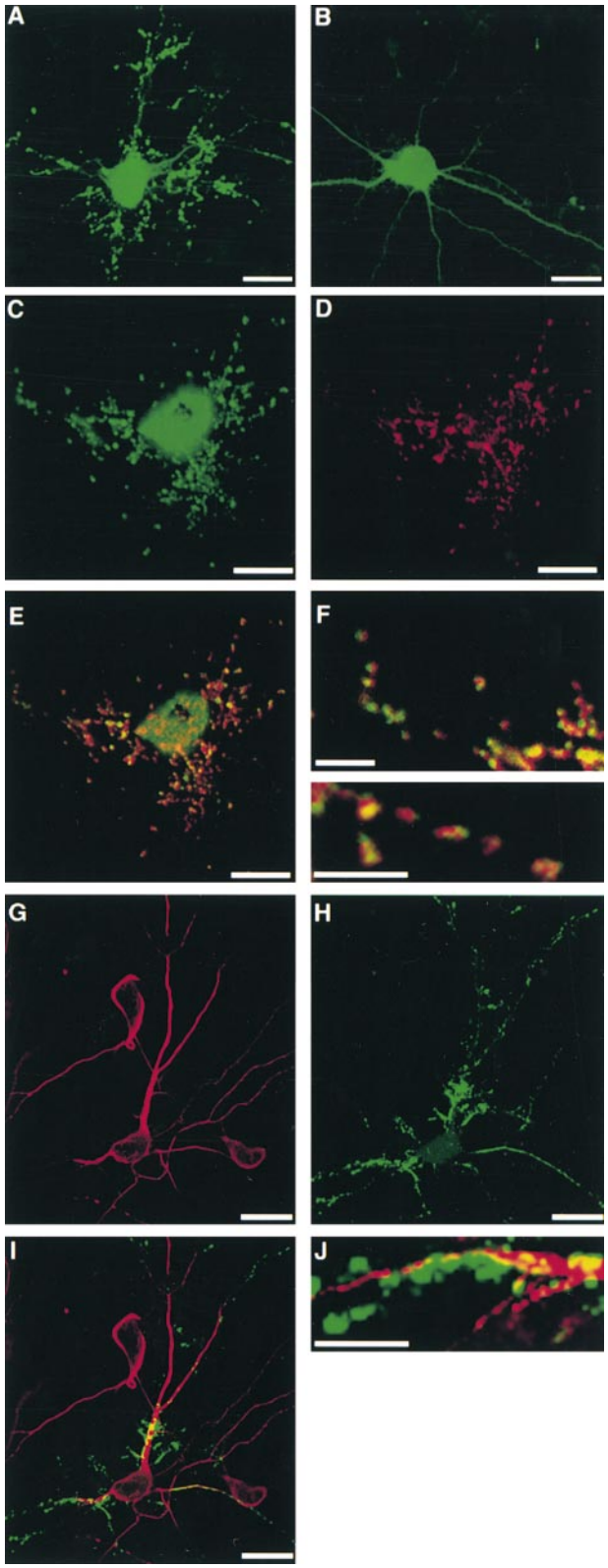

Figure 3. Syndecan-2–dependent clustering of synbindin in dendrites. (A and B) Hippocampal neurons were transfected at 1 DIV with synbindin-GFP and intact syndecan-2 (A) or synbindin-GFP alone (B) and examined at 8 DIV on a confocal microscopy. Note that without cotransfection of syndecan-2, synbindin-GFP is localized diffusely within neurons (B). With cotransfection, synbindin-GFP shows punctate distribution along dendrites (A). (C–F) Hippocampal neurons cotransfected with synbindin-GFP and syndecan-2 were immunostained with anti–syndecan-2 antibody. (C, green) Synbindin-GFP; (D, red) syndecan-2; (E and F) superimposed views. Note that punctate immunoreactivities of synbindin-GFP overlap with syndecan-2 immunoreactive puncta. (G–J) Hippocampal neurons cotransfected with synbindin-GFP and syndecan-2 were immunostained with anti-MAP2 antibody. (H, green) Synbindin-GFP; (G, red) MAP2; (I and J) superimposed views. Note that synbindin-GFP clusters are present along MAP2-positive dendrites. Bars: (A–E and G–I) 20 μm; (F and J) 10 μm.

bindin directly interacts with syndecan-2 through the EFYA tail of syndecan-2, and that the PDZ-like segment of synbindin is involved primarily in the interaction with syndecan-2.

Syndecan-2–dependent Translocation of Synbindin in Hippocampal Neurons

To examine further the physiological significance of the synbindin–syndecan-2 interaction in neurons, we tested whether these two proteins interact in the cytoplasmic environment of cultured hippocampal neurons. For this, hippocampal neurons at 1 DIV were transfected with synbindin-GFP fusion protein alone or together with syndecan-2. The localization of synbindin and syndecan-2 was examined at 8 DIV by GFP signals and immunofluorescence with anti–syndecan-2 antibody, respectively. At this stage in culture, endogenous syndecan-2 is not yet expressed by hippocampal neurons. Therefore, the syndecan-2 immunoreactivities detected in these experiments represent transfected syndecan-2 (Ethell and Yamaguchi, 1999). We found that the distribution of synbindin changes dependent on cotransfection of syndecan-2. In neurons transfected with synbindin-GFP alone, synbindin was distributed diffusely in cytoplasm (Fig. 3 B). In contrast, when neurons were transfected with synbindin-GFP together with intact syndecan-2, synbindin formed clusters along dendrites (Fig. 3 A). Immunostaining of these double-transfected neurons with anti–syndecan-2 antibody demonstrated colocalization of synbindin and syndecan-2 (Fig. 3, C–F). These results demonstrate that not only does synbindin colocalize with syndecan-2 in transfected hippocampal neurons, but also that syndecan-2 induces synbindin clustering in dendrites.

To determine the localization of the synbindin clusters, we performed a series of double labeling experiments. These experiments demonstrated that the synbindin clusters observed in synbindin/syndecan-2 double-transfected neurons are localized in dendritic spines. As shown in Fig. 3, double staining with anti-MAP2 antibody demonstrated that the clusters of synbindin-GFP are localized in small protrusions along dendrites (Fig. 3, G–J). Double staining with the anti–synapsin I antibody revealed that synbindin clusters exhibit partial overlap with synapsin I immunoreactivities (Fig. 4, A–D), a pattern typically seen for postsynaptic proteins (Niethammer et al., 1998; Ethell and Yamaguchi, 1999).

To examine if this clustering of synbindin is mediated by the interaction with the EFYA tail of syndecan-2, as demonstrated by biochemical binding studies, the same double transfection experiments were performed with the syndecan-2ΔEFYA deletion mutant. As shown in Fig. 4, synbin-

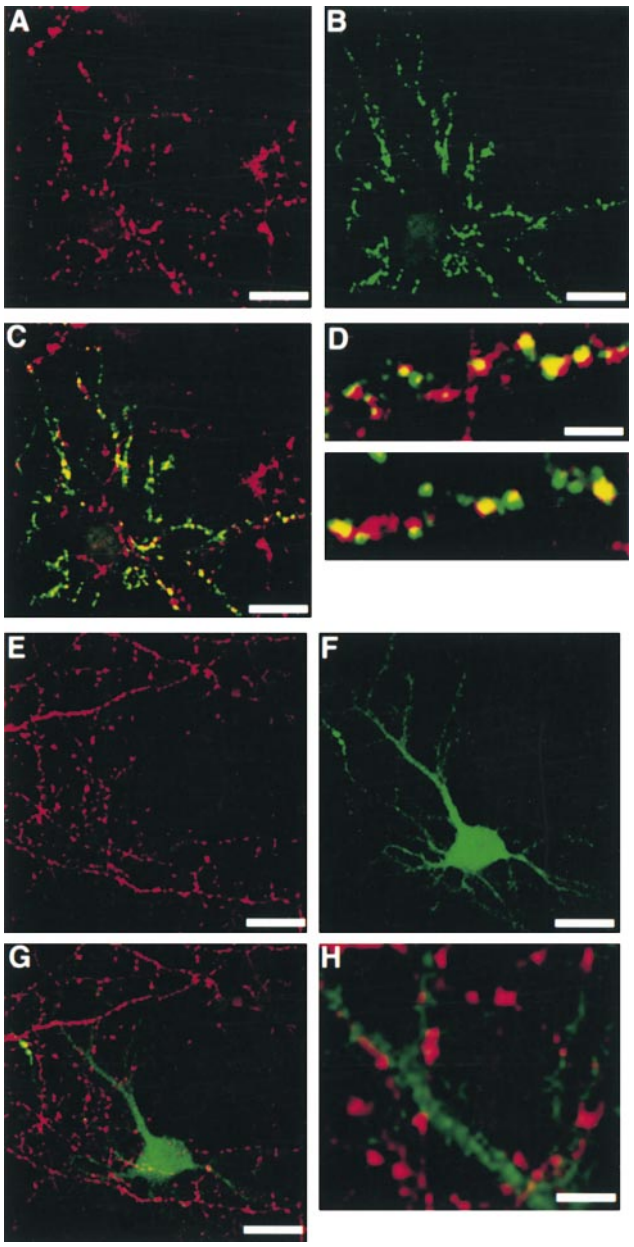

Figure 4. Syndecan-2–mediated clustering of synbindin requires the COOH-terminal EFYA motif. (A–D) Hippocampal neurons cotransfected with synbindin-GFP and intact syndecan-2 were immunostained with anti–synapsin I antibody. Cells were examined at 8 DIV for the distribution of synbindin (visualized with GFP fluorescence) and synapsin I (visualized with RITC-labeled secondary antibody) on a confocal microscopy. (A, red) Synapsin I; (B, green) synbindin-GFP; and (C and D) superimposed views. Note that synbindin-GFP exhibits a partial overlapping with synapsin I puncta along dendrites. (E–H) Hippocampal neurons were cotransfected with synbindin-GFP and the syndecan-2ΔEFYA deletion mutant, and were examined as described above. (E, red) Synapsin I; (F, green) synbindin-GFP; (G and H) superimposed views. Note that synbindin-GFP is distributed diffusely in dendritic shafts and the cell body without clustering. No overlapping with synapsin I puncta are observed. Bars: (A–C and E–G) 20 μm; (D and H) 10 μm.

din failed to cluster in neurons double-transfected with synbindin-GFP and the syndecan-2ΔEFYA mutant (Fig. 4, E–H). In the syndecan-2/synbindin-GFP–cotransfected

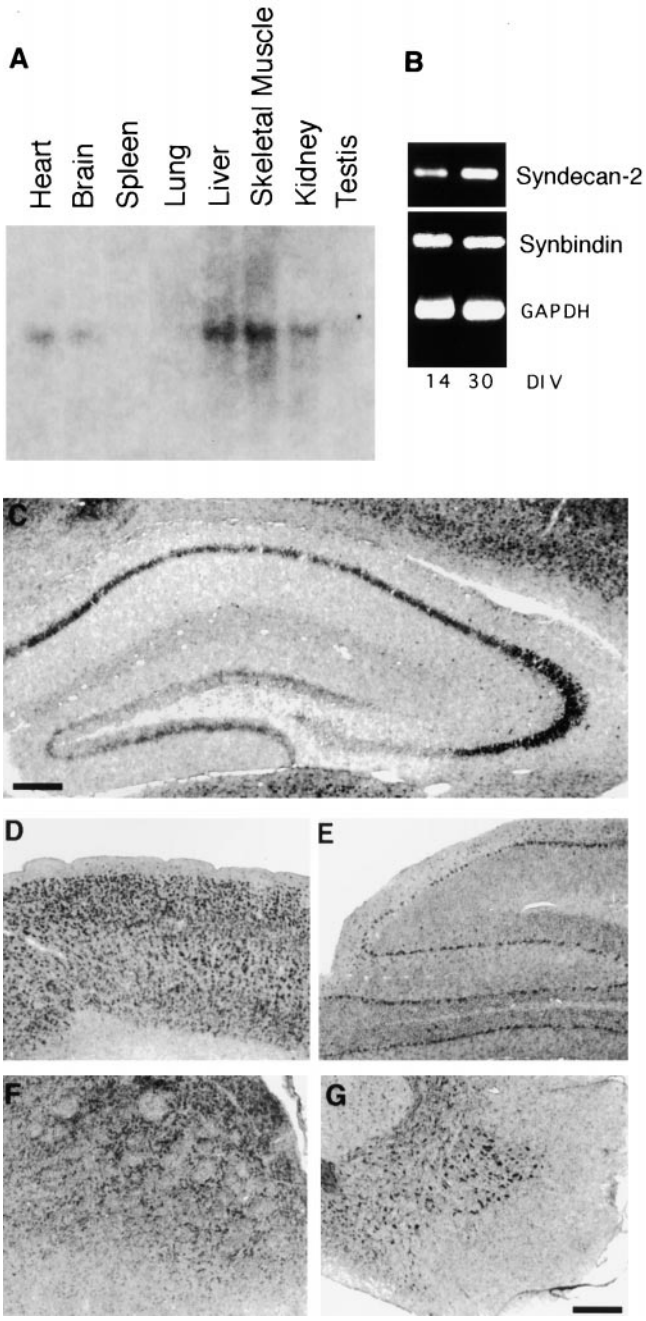

Figure 5. Expression of synbindin mRNA. (A) Northern blot analysis for synbindin expression in adult mouse tissues. (B) RT-PCR analysis for synbindin expression in cultured rat hippocampal neurons at 14 and 30 DIV. GAPDH, glyceraldehyde 3-phosphate dehydrogenase. (C–G) In situ hybridization of synbindin in adult mouse CNS. (C) Hippocampal formation; (D) cerebral cortex; (E) cerebellar cortex; (F) caudate putamen; (G) anterior horn of the spinal cord. Bars: (C) 200 μm; (D–G) 350 μm.

cultures, the majority (83 ± 7%) of GFP-positive neurons showed extensive clustering (>10 clusters per cell) of synbindin-GFP, whereas no cells (0%) were found to contain >3 GFP clusters in the syndecan-2ΔEFYA/synbindin-GFP–cotransfected cultures. We previously demonstrated that the syndecan-2ΔEFYA mutant is expressed and forms clusters in the same manner as the intact syndecan-2 in hippocampal neurons (Ethell and Yamaguchi, 1999).

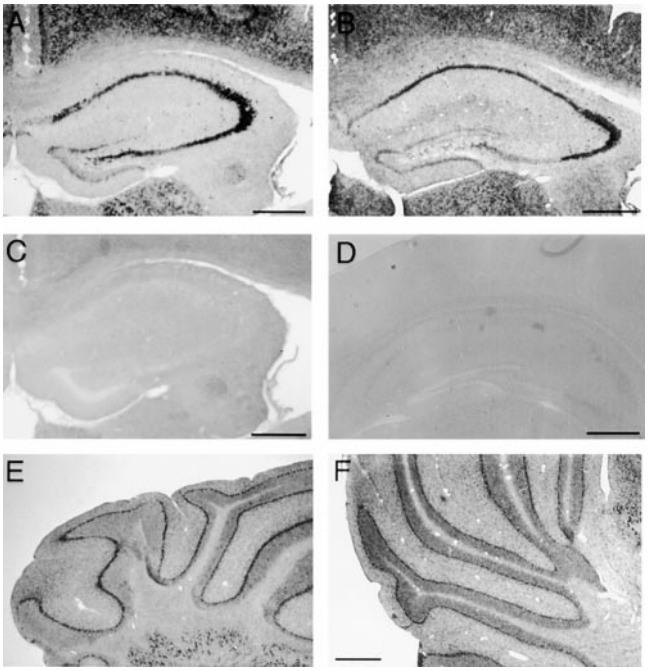

Figure 6. Synbindin and syndecan-2 are expressed in the same types of neurons in adult brain. In situ hybridization was performed as described in Materials and Methods for syndecan-2 (A and E) and synbindin (B and F). C and D show the results of hybridization with control (sense) probes for syndecan-2 and synbindin, respectively. (A–D) Hippocampal formation; (E and F) cerebellum. Note that the expression patterns of syndecan-2 and synbindin are almost identical. Bars, 500 μm.

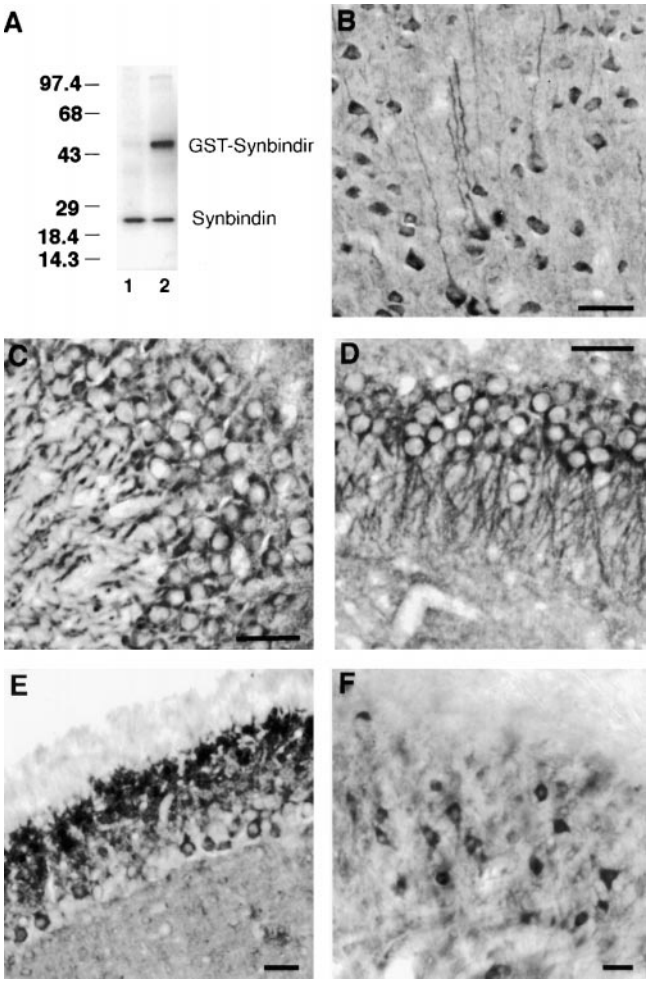

Figure 7. Immunohistochemical localization of synbindin in the adult brain. (A) Identification of synbindin protein in adult brain. The total brain extracts (lane 1) and bacterially produced GST-synbindin fusion proteins (lane 2) were immunoblotted with affinity-purified antisynbindin polyclonal antibody. (B–F) Immunoperoxidase staining for synbindin in the adult mouse brain. (B) Cerebral cortex; (C) CA3 of the hippocampus; (D) CA1 of the hippocampus; (E) cerebellar cortex; (F) deep cerebellar nuclei. Bars, 50 μm.

Therefore, the lack of synbindin clustering in syndecan-2ΔEFYA/synbindin-GFP–cotransfected neurons is not due to the aberrant expression of the syndecan-2ΔEFYA mutant. Taken together, these transfection experiments provide further evidence for the synbindin–syndecan-2 interaction through the EFYA tail of syndecan-2, and suggest that syndecan-2 induces the clustering of synbindin in dendrites.

Expression of Synbindin mRNA in the Nervous System

Northern blotting revealed a 4.4-kb transcript of synbindin that is widely expressed in adult mouse tissues (Fig. 5 A). Such an expression pattern is similar to those of syntenin and CASK (Grootjans et al., 1997; Cohen et al., 1998). RT-PCR and in situ hybridization studies demonstrated that synbindin is strongly expressed in neurons. RT-PCR analysis demonstrated that synbindin mRNA is expressed in cultured hippocampal neurons at 14 and 30 DIV (Fig. 5 B), as was previously shown for syndecan-2 (Ethell and Yamaguchi, 1999). In situ hybridization in the adult mouse central nervous system (CNS) showed that synbindin is expressed predominantly in large neurons. In the cerebrum, strong synbindin expression was observed in pyramidal neurons in the CA1-CA3 regions of hippocampus (Fig. 5 C), pyramidal neurons in the cortex (Fig. 5 D), and large neurons in the caudate putamen (Fig. 5 F). In the cerebellum, Purkinje cells and neurons in the deep cerebellar nuclei exhibited strong synbindin expression (Fig. 5 E). Motor neurons in the spinal cord also showed strong synbindin expression (Fig. 5 G). In contrast, synbindin expression in smaller, granule-type neurons was much weaker or undetectable, including granule neurons in the dentate gyrus (Fig. 5 C) and those in the granular layer of the cerebellar cortex (Fig. 5 E). Throughout the CNS, no synbindin expression was detected in glial cell types. Taken together, these observations suggest that, in the nervous system, synbindin is expressed predominantly by large, pyramidal-type neurons, which tend to have highly developed dendritic arbors.

We compared spatial expression patterns of synbindin and syndecan-2 by in situ hybridization in serial sections. This analysis revealed that these two molecules exhibit almost identical expression patterns in the adult mouse brain. In the hippocampus, syndecan-2 mRNA was detected in pyramidal cells, whereas granule cells of the dentate gyrus exhibited much weaker signals (Fig. 6 A). In the cerebellum, Purkinje cells express syndecan-2, but little

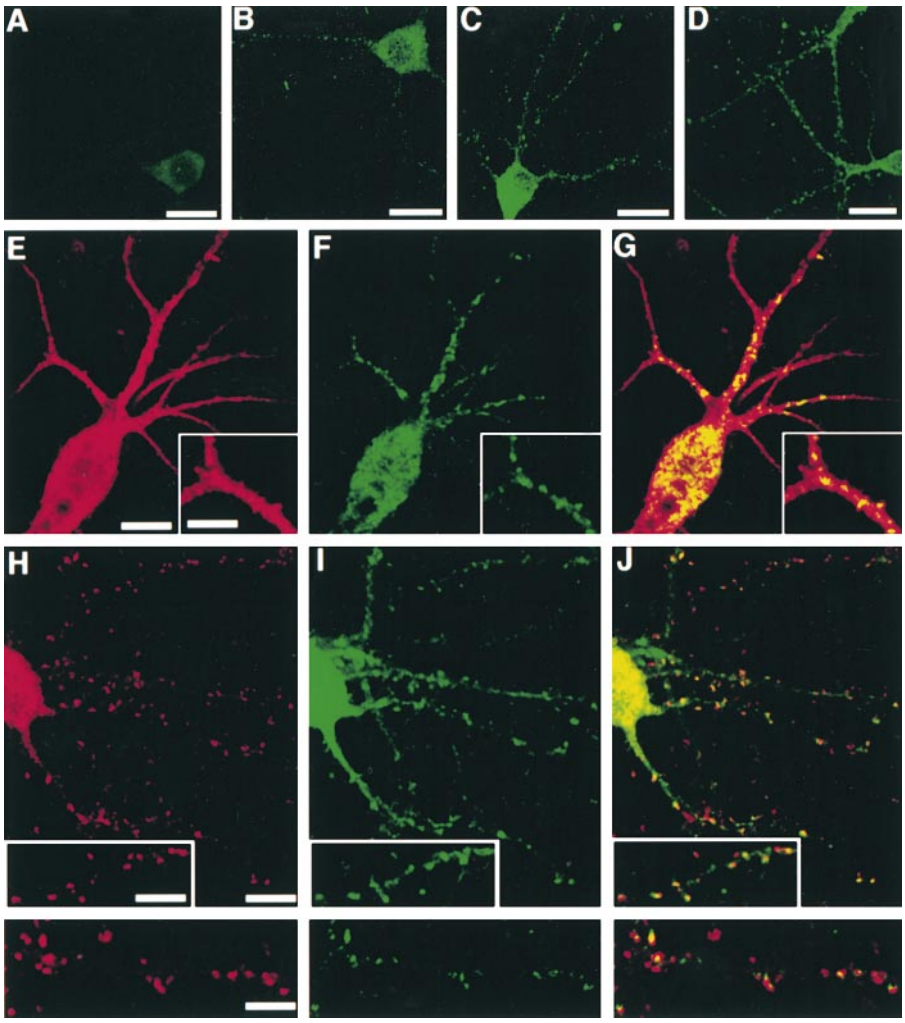

Figure 8. Localization of endogenous synbindin in dendritic spines of cultured hippocampal neurons. (A–D) Accumulation of synbindin in dendritic spines of hippocampal neurons. Hippocampal neurons were stained with affinity-purified antisynbindin antibodies at 7 (A), 14 (B), 21 (C), and 28 (D) DIV. (E–G) Double immunostaining of 30 DIV hippocampal neurons with anti-MAP2 (E) and antisynbindin (F) antibodies, and their superimposed image (G). High magnification views (insets) show that synbindin signals (green) coincide with small protrusions along MAP-2 positive (red) dendritic shafts. (H–J) Double immunostaining of 30 DIV hippocampal neurons with antisynaptophysin (H) and antisynbindin (I) antibodies and their superimposed image (J). High magnification views (insets and bottom panels) show that synbindin immunoreactivities (green) are in close apposition with synaptophysin puncta (red), which is a pattern typical of postsynaptic proteins. Bars: (A–D) 20 μm; (E–J) 10 μm; (insets) 5 μm.

syndecan-2 expression was observed in granule neurons (Fig. 6 E). This spatial expression pattern is very similar to that of synbindin (Fig. 6, B and F).

Immunohistochemical Identification of Synbindin In Vivo

To investigate the localization of endogenous synbindin in vivo, we generated polyclonal antisera to synbindin. Antibodies affinity-purified from this antiserum reacted with a 24-kD band in adult mouse brain extracts (Fig. 7 A, lane 1), which comigrate with synbindin released from GST-synbindin (lane 2). In tissue sections, synbindin immunoreactivities were observed in various neurons in the adult mouse brain. Strong immunoreactivities were found in pyramidal neurons of the cerebral cortex (Fig. 7 B), pyramidal neurons of the hippocampus (Fig. 7, C and D), Purkinje cells of the cerebellum (Fig. 7 E), and neurons of the deep cerebellar nucleus (Fig. 7 F). In general, this result is consistent with the expression pattern of synbindin mRNA demonstrated by in situ hybridization (Fig. 5). Synbindin immunoreactivities were mainly associated with the soma and the apical dendrites of these neurons. In the hippocampus, strong immunoreactivities were observed in the stratum lucidum where the dendrites of CA3 pyramidal neurons are present (Fig. 7 C). In the cerebellum, the cell bodies and apical dendrites of Purkinje neurons were intensely labeled (Fig. 7 E).

Accumulation of Endogenous Synbindin in Spines of Cultured Hippocampal Neurons

We have shown previously that endogenous syndecan-2 is concentrated in dendritic spines of cultured hippocampal neurons after 2 wk in vitro (Ethell and Yamaguchi, 1999). Immunocytochemistry revealed that synbindin exhibits a similar temporal expression pattern in dendritic spines (Fig. 8). At 7 DIV, synbindin immunoreactivity was detected diffusely in the cytoplasm of the soma (Fig. 8 A). No punctate immunoreactivity was detected at this stage. At 14 DIV, punctate immunoreactivity became apparent along the dendrites (Fig. 8 B). The intensity of the punctate staining grew stronger at 21 and 28 DIV (Fig. 8, C and D). This time course is similar to that of syndecan-2 expression in dendritic spines and that of the spine morphogenesis in this culture system (Ethell and Yamaguchi, 1999). Double immunostaining of 30 DIV hippocampal neurons confirmed the presence of endogenous synbindin in dendritic spines (Fig. 8, E–J). Synbindin immunoreactivities correspond to small protrusions along MAP2-positive dendritic

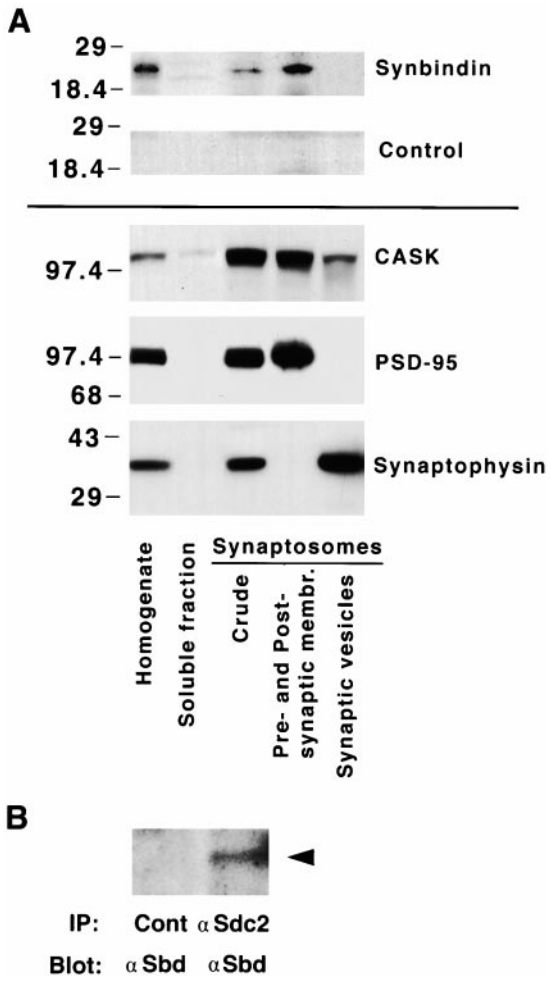

Figure 9. Subcellular distribution of synbindin and coimmunoprecipitation of endogenous synbindin and syndecan-2. (A) Subcellular fractions were prepared from adult mouse cerebral cortex as described in Materials and Methods. Equal amounts of proteins from each fraction were resolved in a 8–16% gel and immunoblotted with antisynbindin antibody, preimmune serum (control), anti-CASK, anti–PSD-95, or antisynaptophysin antibody. (B) Synbindin coimmunoprecipitates with syndecan-2 from the synaptic membrane fraction. Materials immunoprecipitated from the synaptic membrane fraction with anti–syndecan-2 antibodies and protein G–agarose (lane 2) or with protein G–agarose only (lane 1) were separated on SDS-PAGE and immunoblotted with antisynbindin antibody (No. 157).

shafts (Fig. 8, E–G). Double staining with antisynbindin and antisynaptophysin antibodies showed a partial overlapping pattern (Fig. 8, H–J), as observed in transfected neurons (Fig. 4, C and D). At high magnification (Fig. 8, insets and bottom panels), synbindin puncta (green) are in close apposition with synaptophysin puncta (red) but do not completely overlap, which is a typical distribution pattern for postsynaptic proteins. Taken together, these results demonstrate that endogenous synbindin molecules in mature neurons exist in dendritic spines, which is consistent with in vitro transfection studies (Figs. 3 and 4).

Unlike syndecan-2, which exhibits essentially no immunoreactivity on dendritic shafts in mature (30 DIV) neurons (Ethell and Yamaguchi, 1999), synbindin was detected within dendritic shafts and neuronal soma (Fig. 8, F and I), even at 30 DIV. This is consistent with the immunohistochemical results in which synbindin immunoreactivities were observed along dendrites and in the soma (Fig. 7). Considering that synbindin has similarities with proteins involved in membrane trafficking, it is suspected that synbindin may also associate with intracellular membrane compartments within dendrites and cell bodies.

Endogenous Synbindin Is Enriched in Synaptic Membranes and Associated with Syndecan-2

To characterize the subcellular localization of synbindin, we prepared subcellular fractions from adult mouse cortex using a differential centrifugation procedure (Li et al., 1996; Wang et al., 1997). Two marker proteins, PSD-95 (postsynaptic marker) and synaptophysin (synaptic vesicle marker), were used as controls. Synbindin was fractionated into the crude synaptosome fraction and further enriched in the synaptic membrane fraction (Fig. 9 A). The fractionation pattern of synbindin was similar to that of PSD-95. These results indicate that synbindin is associated with synapses.

To obtain in vivo biochemical evidence for the synbindin–syndecan-2 interaction, we examined whether endogenous synbindin and syndecan-2 coprecipitate from brain extracts. As shown in Fig. 9 B, anti–syndecan-2 mAb precipitated synbindin from the CHAPS extracts of the synaptic membrane fraction. Taken together, these results provide further evidence for the synbindin-syndecan-2 interaction in vivo.

Ultrastructural Localization of Synbindin in Synapses and Intracellular Organelles

To determine the precise intracellular localization of synbindin in vivo, we performed immunogold electron microscopy in the adult mouse cerebral cortex. This analysis demonstrated synbindin immunolabeling in two distinct structures in neurons, synapses, and intracellular membrane organelles. Immunogold labeling for synbindin was concentrated at asymmetric synapses (Fig. 10, A–D). Labeling was seen on both pre- and postsynaptic membranes, but the majority of the labeling was on the postsynaptic side in close association with postsynaptic membranes. Quantitative analysis of the distribution of gold particles confirmed that synbindin is concentrated on the postsynaptic side of synapses (Fig. 10 G). Such a distribution pattern of synbindin is consistent with that of syndecan-2, as determined by immunogold labeling (Hsueh et al., 1998).

Immunogold labeling demonstrated that synbindin is also associated with membrane-bound compartments within neurons (Fig. 10, H–J). Consistent with the light microscopic findings (Fig. 7), immunogold labeling for synbindin was observed in the soma and dendritic shafts of cortical neurons. In these sites, labeling was associated predominantly with various cisterns and vesicles. Dense labeling was observed on the Golgi apparatus (Fig. 10, H and I) and unidentified vesicles in the dendritic shaft (Fig. 10 J). Membrane compartments within dendritic spines

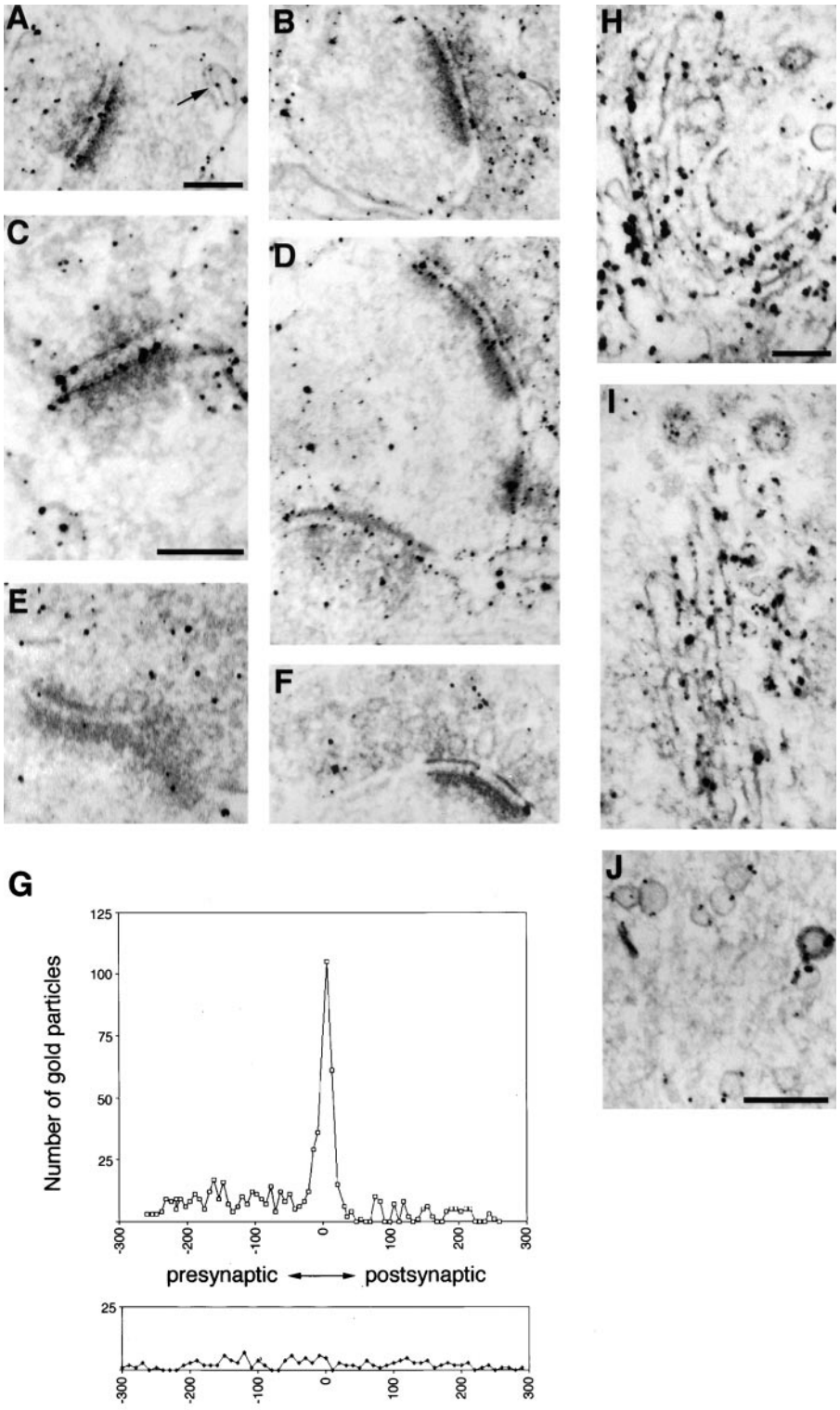

Figure 10. Immunogold localization of synbindin in neurons of the adult rat cerebral cortex. (A–F) Immunogold electron microscopy of asymmetric synapses in the adult mouse cerebral cortex. (A–D) Labeling with affinity-purified antisynbindin antibody. (E and F) Negative controls labeled with preimmune antibody. Note that synbindin immunoreactive gold particles are concentrated in synapses, mainly on the postsynaptic membranes. Membrane cisterns and vesicles within dendritic spines are also labeled (A, arrow). (G) Quantitative analysis of the distribution of synbindin immunoreactive gold particles. The horizontal axis represents the distance in nanometers from the middle of the synaptic cleft (zero point). The peak of the chart coincides with the postsynaptic membrane. Note that the highest concentrations of gold particles coincide with the postsynaptic membrane and PSD. The bottom panel shows the background distribution of gold particles in the control sections. (H–J) Immunogold electron microscopy of intracellular membrane compartments in the neurons of the adult mouse cerebral cortex. (H and I) Golgi apparatus in the soma and dendritic shaft. (J) Unidentified vesicles in the dendritic shaft. Bars, 0.1 μm.

were also labeled (Fig. 10 A, arrow). These observations demonstrate that synbindin is indeed associated with intracellular cisterns and vesicles, supporting the notion that synbindin is involved in vesicular transport and membrane trafficking in dendrites. Thus, these immunoelectron microscopy results indicate that synbindin is localized in two distinct subcellular structures in neurons: (1) synapses (mainly postsynaptic membranes and PSD) and (2) intracellular membrane cisterns. Similar dual localization has been reported for other cytoplasmic proteins implicated in synaptic functions, including GRIP1 (Dong et al., 1999) and α-actinin-2 (Wyszynski et al., 1998).

Discussion

In previous work, we demonstrated that syndecan-2 induces the formation of morphologically mature dendritic spines, and that this effect is mediated by the cytoplasmic interaction through the COOH terminus of syndecan-2 (Ethell and Yamaguchi, 1999). We report here a novel syndecan-2-binding protein, synbindin. Our results indicate that synbindin is a postsynaptic protein that is likely to be involved in intracellular vesicle transport in dendritic spines. This suggests a possibility that syndecan-2 exerts its effects on spine morphogenesis by recruiting synbindin-positive membrane cisterns toward postsynaptic sites.

Synbindin, A Novel Syndecan-2–binding Protein in Neurons

Synbindin is the third molecule, after syntenin (Grootjans et al., 1997) and CASK (Cohen et al., 1998; Hsueh et al., 1998), that has been shown to bind the COOH terminus of syndecan-2. Both syntenin and CASK contain PDZ domains and bind syndecan-2 through these domains. Synbindin has a segment that shares homologies with PDZ domains, and this segment is primarily involved in binding to syndecan-2. However, this segment does not constitute a classical PDZ domain. It remains to be determined whether the synbindin–syndecan-2 interaction can be explained according to the well-established paradigm of the recognition of protein COOH termini by PDZ domains. Yet, the fact that proteins that bear homology with this segment of synbindin are predominantly PDZ domain proteins suggests that synbindin has some remote structural relationships with this family of proteins.

On the other hand, synbindin has clear structural relationships with proteins involved in vesicular transport and membrane trafficking. Synbindin exhibits 43% homology with a yeast protein, tentatively named p23 (Sacher et al., 1998), which has been identified as a component of multiprotein complex called TRAPP (Sacher et al., 1998). In yeast cells, the TRAPP complex is thought to mediate the docking and fusion of ER-to-Golgi transport vesicles. Bet5p, which has sequence homology with synbindin (Fig. 1), is also a component of the TRAPP complex (Sacher et al., 1998). These observations suggest that synbindin is involved in membrane trafficking in neurons. Consistent with this possibility, immunoelectron microscopy demonstrated that synbindin is present on membrane-bound cisterns and vesicles within the soma and dendrites of cortical neurons. Thus, it is likely that synbindin is involved in membrane trafficking in neurons.

Physiological Significance of the Interaction

Despite the fact that the synbindin-syndecan-2 interaction may not be explained by the well-established paradigm of the interaction between PDZ domains and protein COOH termini, there is ample evidence for the physiological significance of the interaction. In situ hybridization and immunohistochemistry demonstrated that, in the CNS, synbindin is expressed by certain neuronal populations, most notably large, pyramidal-type neurons. In contrast, synbindin expression is weak in granular-type neurons, such as the neurons of the dentate gyrus and the granular layer of the cerebellum. This pattern of expression is very similar to that of syndecan-2 (Fig. 6). In mature hippocampal neurons in culture, synbindin is concentrated in dendritic spines, as previously shown for syndecan-2 (Ethell and Yamaguchi, 1999). Cotransfection experiments showed that syndecan-2 causes the clustering of synbindin in dendritic spines, and that this syndecan-2–dependent clustering of synbindin occurs through the EFYA tail of syndecan-2. These results indicate that the synbindin–syndecan-2 interaction occurs in the cytoplasmic environment of hippocampal neurons with the same specificity as observed in two-hybrid assays. By immunogold electron microscopy and biochemical fractionation, we demonstrated that synbindin is associated with synaptic membranes, mainly at the postsynaptic side, where the existence of syndecan-2 has been reported previously (Hsueh et al., 1998; Hsueh and Sheng, 1999). Finally, synbindin coimmunoprecipitates with syndecan-2 from the synaptic membrane fractions. These results strongly suggest that synbindin and syndecan-2 interact physiologically in dendritic spines of certain populations of neurons.

Clustering of Synbindin in Dendritic Spines Requires Syndecan-2

In the previous study, we showed that the interaction of the syndecan-2 and its cytoplasmic ligands is essential for transfected syndecan-2 to induce spine formation (Ethell and Yamaguchi, 1999). Furthermore, our work demonstrated that the cytoplasmic syndecan-2 ligands essential for spine formation are recruited by syndecan-2 rather than the cytoplasmic ligands recruit syndecan-2 (Ethell and Yamaguchi, 1999). The sorting behavior of transfected synbindin in hippocampal neurons is consistent with the following observation: the clustering of synbindin in spines requires syndecan-2 expression (Figs. 3 and 4). Moreover, the clustering of endogenous synbindin during the course of hippocampal cultures is also consistent with this notion: the clustering of synbindin in spines occurs after 2 wk in vitro, coinciding with the accumulation of syndecan-2 in spines (Ethell and Yamaguchi, 1999). These results indicate that syndecan-2 recruits cytoplasmic proteins to the membrane sites that later become dendritic spines. Thus, syndecan-2 may act as a mediator of extracellular signals, which specify the site of prospective dendritic spines, though we have not determined if any extracellular ligands are involved in the syndecan-2 action on spine morphogenesis. In this vein, it is interesting to examine whether other intracellular syndecan-2 ligands, namely CASK and syntenin, are also translocated to spines dependent on the expression of syndecan-2. If so, the role of syndecan-2 may be a more general one.

Possible Role of Synbindin in Dendritic Spine Morphogenesis

Our previous work showed that a molecule that binds to the syndecan-2 EFYA tail plays a crucial role in the process of syndecan-2–induced spine formation as a downstream effector (Ethell and Yamaguchi, 1999); however, it is not known which molecule among the three known EFYA ligands (syntenin, CASK, and synbindin) is relevant to this process. Some of these interactions may turn

out to be irrelevant to spine formation. On the other hand, it is possible that all three interactions occur in neurons, as they are all expressed in neurons (Hsueh et al., 1998; Ethell and Yamaguchi, 1999). It is also possible that these molecules play different roles within neurons. Having PDZ domains, CASK and syntenin are likely to be involved in the assembly of the cytoskeletal scaffold. Lacking the classical PDZ domain and other cytoskeletal motifs, synbindin is unlikely to be involved in the assembly of the postsynaptic cytoskeletal scaffold. On the other hand, the homology with the components of the yeast TRAPP complex suggests synbindin is involved in vesicle transport in neurons.

There is increasing evidence that membrane trafficking plays an important role in functional maturation of postsynaptic structures. For instance, Lledo et al. (1998) showed that inhibition of membrane trafficking with the botulinum toxin suppresses LTP. In dendritic spines, AMPA receptors are present in association with intracellular vesicles, and upon stimulation of synapses, these AMPA-containing vesicles dock and fuse with the postsynaptic plasma membrane (Nusser et al., 1998; Shi et al., 1999). Membrane fusion in postsynaptic sites is thought to be mediated by *N*-ethylmaleimide-sensitive fusion protein and SNAREs (Turner et al., 1999). Interestingly, there is evidence that the TRAPP complex acts upstream of the SNARE complex assembly. Rossi et al. (1995) showed that the SNARE complex does not form in the yeast *BET3* mutant, indicating that BET3 genetically interacts with the SNARE pathway. As discussed above, both BET3 and p23, the putative yeast homologue of synbindin, are components of the TRAPP complex (Sacher et al., 1998). This suggests that synbindin is involved in membrane trafficking in postsynaptic sites.

At present, we do not know whether synbindin acts as a downstream effector in the syndecan-2–induced spine formation. Yet, there are a few possible scenarios that synbindin is involved in the process of spine formation. Dendritic spines contain membrane-bound organelles (Villa et al., 1992; Spacek and Harris, 1997; Gardiol et al., 1999). These organelles, or spine apparatus, appear throughout the spine and are sometimes seen around the lateral margins of the postsynaptic density (Harris and Stevens, 1988; Spacek and Harris, 1997). These membrane-bound organelles are thought to play important roles in local synthesis and posttranslational modification of neurotransmitter receptors. Therefore, synbindin clustering induced by syndecan-2 expression may facilitate local synthesis and transport of neurotransmitter receptors. This may, in turn, result in an increase in synaptic efficiency and early maturation of postsynaptic structures. Another possibility, which we currently favor, is that the synbindin–syndecan-2 interaction promotes the recruitment of Ca^{2+}-storing membrane compartments toward synapses, and the Ca^{2+} mobilization from these compartments induces morphological changes of spines. Membrane cisterns immunoreactive for inositol trisphosphate and/or ryanodine receptors, which identify intracellular Ca^{2+} stores, have been shown in dendritic spines, sometimes in the close vicinity of postsynaptic membranes (Sharp et al., 1993; Berridge, 1998; Fagni et al., 2000). Moreover, a moderate and transient increase in $[Ca^{2+}]$ due to release from these Ca^{2+} stores has been shown to cause elongation of existing spines and the formation of new ones (Korkotian and Segal, 1999; Segal et al., 2000). These observations suggest that morphogenesis of dendritic spines involves the recruitment of Ca^{2+}-storing vesicles in the vicinity of synapses. Therefore, the induction of spine formation by syndecan-2 may be due to the recruitment of synbindin-coated Ca^{2+}-storing membrane compartments toward subsynaptic locations. In any event, the identification of a protein that is involved in vesicle transport as a ligand for a cell-surface proteoglycan suggests that extracellular cues may have a role in determining the destination of these vesicles over dendritic surfaces, which in turn promotes the formation of postsynaptic specialization at such a destination.

We thank Drs. Merton Bernfield, Andrew Czernik, Guido David, and Morgan Sheng for their gifts of antibodies, Drs. Andreas Zisch and Elena Pasquale for their help in yeast two-hybrid screening, Dr. E. Monosov for his advice on confocal imaging, Jo Dee Fish for technical assistance with EM, and Dr. Mary E.T. Boyle for critical reading of the manuscript.

This work was supported by the National Institutes of Health grant HD25938 to Y. Yamaguchi.

Submitted: 15 March 2000
Revised: 10 July 2000
Accepted: 15 August 2000

References

Belliveau, D.J., I. Krivko, J. Kohn, C. Lachance, C. Pozniak, D. Rusakov, D. Kaplan, F.D. Miller. 1997. NGF and neurotrophin-3 both activate TrkA on sympathetic neurons but differentially regulate survival and neuritogenesis. *J. Cell Biol.* 136:375–388.

Bernfield, M., R. Kokenyesi, M. Kato, M.T. Hinkes, J. Spring, R.L. Gallo, E.J. Lose. 1992. Biology of the syndecans: a family of transmembrane heparan sulfate proteoglycans. *Annu. Rev. Cell Biol.* 8:365–393.

Berridge, M.J. 1998. Neuronal calcium signalling. *Neuron*. 21:13–26.

Bondareff, W. 1967. An intercellular substance in rat cerebral cortex: submicroscopic distribution of ruthenium red. *Anat. Rec.* 157:527–535.

Carey, D.J. 1997. Syndecans: multifunctional cell-surface co-receptors. *Biochem. J.* 327:1–16.

Carey, D.J., R.C. Stahl, B. Tucker, K.A. Bendt, and G. Cizmeci-Smith. 1994. Aggregation-induced association of syndecan-1 with microfilaments mediated by the cytoplasmic domain. *Exp. Cell Res.* 214:12–21.

Cohen, A.R., D.F. Wood, S.M. Marfatia, Z. Walther, A.H. Chishti, and J.M. Anderson. 1998. Human CASK/LIN-2 binds syndecan-2 and protein 4.1 and localizes to the basolateral membrane of epithelial cells. *J. Cell Biol.* 142: 129–138.

Cole, G.J., and W. Halfter. 1996. Agrin: an extracellular matrix heparan sulfate proteoglycan involved in cell interactions and synaptogenesis. *Perspect. Dev. Neurobiol.* 3:359–371.

Dong, H., R.J. O'Brien, E.T. Fung, A.A. Lanahan, P.F. Worley, and R.L. Huganir. 1997. GRIP: a synaptic PDZ domain-containing protein that interacts with AMPA receptors. *Nature*. 386:279–284.

Dong, H., P. Zhang, I. Song, R.S. Petralia, D. Liao, and R.L. Huganir. 1999. Characterization of the glutamate receptor-interacting proteins GRIP1 and GRIP2. *J. Neurosci.* 19:6930–6941.

Duclos, F., U. Boschert, G. Sirugo, J.L. Mandel, R. Hen, and M. Koenig. 1993. Gene in the region of the Friedreich ataxia locus encodes a putative transmembrane protein expressed in the nervous system. *Proc. Natl. Acad. Sci. USA*. 90:109–113.

Eldridge, C.F., J.R. Sanes, A.Y. Chiu, R.P. Bunge, and C.J. Cornbrooks. 1986. Basal lamina-associated heparan sulphate proteoglycan in the rat PNS: characterization and localization using monoclonal antibodies. *J. Neurocytol.* 15: 37–51.

Ethell, I.M., and Y. Yamaguchi. 1999. Cell-surface heparan sulfate proteoglycan syndecan-2 induces the maturation of dendritic spines in rat hippocampal neurons. *J. Cell Biol.* 144:575–586.

Fagni, L., F. Chavis, F. Ango, and J. Bockaert. 2000. Complex interactions between mGluRs, intracellular Ca^{2+} stores and ion channels in neurons. *Trends Neurosci.* 23:80–88.

Gardiol, A., C. Racca, and A. Triller. 1999. Dendritic and postsynaptic protein synthetic machinery. *J. Neurosci.* 19:168–179.

Grootjans, J.J., P. Zimmermann, G. Reekmans, A. Smets, G. Degeest, J. Durr, and G. David. 1997. Syntenin, a PDZ protein that binds syndecan cytoplas-

mic domains. *Proc. Natl. Acad. Sci. USA*. 94:13683–13688.
Hall, Z.W., and J.R. Sanes. 1993. Synaptic structure and development: the neuromuscular junction. *Cell*. 72(Suppl):99–121.
Harris, K.M., and J.K. Stevens. 1988. Dendritic spines of rat cerebellar Purkinje cells: serial electron microscopy with reference to their biophysical characteristics. *J. Neurosci.* 8:4455–4469.
Harris, K.M., and S.B. Kater. 1994. Dendritic spines: cellular specializations imparting both stability and flexibility to synaptic function. *Annu. Rev. Neurosci.* 17:341–371.
Hsueh, Y.P., and M. Sheng. 1999. Regulated expression and subcellular localization of syndecan heparan sulfate proteoglycans and the syndecan-binding protein CASK/LIN-2 during rat brain development. *J. Neurosci.* 19:7415–7425.
Hsueh, Y.P., F.C. Yang, V. Kharazia, S. Naisbitt, A.R. Cohen, R.J. Weinberg, and M. Sheng. 1998. Direct interaction of CASK/LIN-2 and syndecan heparan sulfate proteoglycan and their overlapping distribution in neuronal synapses. *J. Cell Biol.* 142:139–151.
Jiang, Y., A. Scarpa, L. Zhang, S. Stone, E. Feliciano, and S. Ferro-Novick. 1998. A high copy suppresser screen reveals genetic interactions between BET3 and a new gene. Evidence for a novel complex in ER-to-Golgi transport. *Genetics.* 149:833–841.
Kim, C.W., O.A. Goldberger, R.L. Gallo, and M. Bernfield. 1994. Members of the syndecan family of heparan sulfate proteoglycans are expressed in distinct cell-, tissue-, and development-specific patterns. *Mol. Biol. Cell.* 5:797–805.
Korkotian, E., and M. Segal. 1999. Release of calcium from stores alters the morphology of dendritic spines in cultured hippocampal neurons. *Proc. Natl. Acad. Sci. USA*. 96:12068–12072.
Li, X.J., A.H. Sharp, S.H. Li, T.M. Dawson, S.H. Snyder, and C.A. Ross. 1996. Huntington-associated protein (HAP1): discrete neuronal localizations in the brain resemble those of neuronal nitric oxide synthase. *Proc. Natl. Acad. Sci. USA*. 93:4839–4844.
Lledo, P.-M., X. Zhang, T.C. Südhof, R.C. Malenka, and R.A. Nicoll. 1998. Postsynaptic membrane fusion and long-term potentiation. *Science.* 279:399–403.
Lories, V., J.J. Cassiman, H. Van der Berghe, and G. David. 1989. Multiple distinct membrane heparan sulfate proteoglycans in human lung fibroblasts. *J. Biol. Chem.* 264:7009–7016.
Meier, T., F. Masciulli, C. Moore, F. Schoumacher, U. Eppenberger, A.J. Denzer, G. Jones, and H.R. Brenner. 1998. Agrin can mediate acetylcholine receptor gene expression in muscle by aggregation of muscle-derived neuregulins. *J. Cell Biol.* 141:715–726.
Murase, S., and E.M. Schuman. 1999. The role of cell adhesion molecules in synaptic plasticity and memory. *Curr. Opin. Cell Biol.* 11:549–553.
Niethammer, M., J.G. Valtschanoff, T.M. Kapoor, D.W. Allison, T.M. Weinberg, A.M. Craig, and M. Sheng. 1998. CRIPT, a novel postsynaptic protein that binds to the third PDZ domain of PSD-95/SAP90. *Neuron.* 20:693–707.
Nusser, Z., R. Lujan, G. Laube, J.D.B. Roberts, E. Molnar, and P. Somogyi. 1998. Cell type and pathway dependence of synaptic AMPA receptor number and variability in the hippocampus. *Neuron*. 21:545–559.
Okamoto, M., and T. Südhof. 1997. Mints, Munc18-interacting proteins in synaptic vesicle exocytosis. *J. Biol. Chem.* 272:31459–31464.
Philipp, S., and V. Flockerzi. 1997. Molecular characterization of a novel human PDZ domain protein with homology to INAD from *Drosophila melanogaster*. *FEBS (Fed. Exp. Biochem. Soc.) Lett.* 413:243–248.
Rapraeger, A.C., and V.L. Ott. 1998. Molecular interactions of the syndecan core proteins. *Curr. Opin. Cell Biol.* 10:620–628.
Rose, S.P.R. 1995. Cell-adhesion molecules, glucocorticoids and long-term-memory formation. *Trends Neurosci.* 18:502–506.
Rossi, G., K. Kolstad, S. Stone, F. Palluault, and S. Ferro-Novick. 1995. BET3 encodes a novel hydrophilic protein that acts in conjunction with yeast SNAREs. *Mol. Biol. Cell.* 6:1769–1780.
Sacher, M., Y. Jiang, J. Barrowman, A. Scarpa, J. Burston, L. Zhang, D. Schieltz, J.R. Yates III, H. Abeliovich, and S. Ferro-Novick. 1998. TRAPP, a highly conserved novel complex on the cis-Golgi that mediates vesicle docking and fusion. *EMBO (Eur. Mol. Biol. Organ.) J.* 17:2494–2503.
Schubert, D. 1991. The possible role of adhesion in synaptic modification. *Trends Neurosci.* 14:127–130.
Segal, M., E. Korkotian, and D.D. Murphy. 2000. Dendritic spine formation and pruning: common cellular mechanism? *Trends Neurosci.* 23:53–57.
Serafini, T. 1999. Finding a partner in a crowd: neuronal diversity and synaptogenesis. *Cell*. 98:133–136.
Shapiro, L., and D.R. Colman. 1999. The diversity of cadherins and implications for a synaptic adhesive code in the CNS. *Neuron*. 23:427–430.
Sharp, A.H., P.H. McPherson, T.M. Dawson, C. Aoki, K.P. Campbell, and S.H. Snyder. 1993. Differential immunohistochemical localization of inositol 1,4,5-trisphosphate- and ryanodine-sensitive Ca^{2+} release channels in rat brain. *J. Neurosci.* 13:3051–3063.
Shi, S.-H., Y. Hayashi, R.S. Petralia, S.H. Zaman, R.J. Wenthold, K. Svoboda, and R. Malinow. 1999. Rapid spine delivery and redistribution of AMPA receptors after synaptic NMDA receptor activation. *Science.* 284:1811–1816.
Spacek, J., and K.M. Harris. 1997. Three-dimensional organization of smooth endoplasmic reticulum in hippocampal CA1 dendrites and dendritic spines of the immature and mature rat. *J. Neurosci.* 17:190–203.
Srivastava, S., P. Osten, F.S. Vilim, L. Khatri, G. Inman, B. States, C. Daly, S. DeSouza, R. Abagyan, J.G. Valtschanoff, R.J. Weinberg, and E.B. Ziff. 1998. Novel anchorage of GluR2/3 to the postsynaptic density by the AMPA receptor-binding protein ABP. *Neuron.* 21:581–591.
Takahashi, H., and T. Tabira. 1999. X11L2, a new member of the X11 protein family, interacts with Alzheimer's β-amyloid precursor protein. *Biochem. Biophys. Res. Commun.* 255:663–667.
Tani, E., and T. Ametani. 1971. Extracellular distribution of ruthenium red-positive substance in the cerebral cortex. *J. Ultrastruct. Res.* 34:1–14.
Torres, R., B.L. Firestein, H. Dong, J. Sraudinger, E.N. Olson, R.L. Huganir, D.S. Bredt, N.W. Gale, and G.D. Yancopoulos. 1998. PDZ proteins bind, cluster, and synaptically colocalize with Eph receptors and their ephrin ligands. *Neuron.* 21:1453–1463.
Tunwell, R.E.A., C. Wickenden, B.M.A. Bertrand, V.I. Shevchenko, M.B. Walsh, P.D. Allen, and F.A. Lai. 1996. The human cardiac muscle ryanodine receptor-calcium release channel: identification, primary structure and topological analysis. *Biochem. J.* 318:477–487.
Turner, K.M., R.D. Burgoyne, and A. Morgan. 1999. Protein phosphorylation and the regulation of synaptic membrane traffic. *Trends Neurosci.* 22:459–464.
Ullmer, C., K. Schmuck, A. Figge, and H. Lubbert. 1998. Cloning and characterization of MUPP1, a novel PDZ domain protein. *FEBS (Fed. Eur. Biochem. Soc.) Lett.* 424:63–68.
Villa, A., A.H. Sharp, G. Racchetti, P. Podini, D.G. Bole, W.A. Dunn, T. Pozzan, S.H. Snyder, and J. Meldolesi. 1992. The endoplasmic reticulum of Purkinje neuron body and dendrites: molecular identity and specializations for Ca^{2+} transport. *Neuroscience.* 49:467–477.
Vojtek, A.B., and S.M. Hollenberg. 1995. Ras-Raf interaction: two-hybrid analysis. *Methods Enzymol.* 255:331–342.
Wang, Y., M. Okamoto, F. Schmitz, K. Hofmann, and T.C. Südhof. 1997. Rim is a putative Rab3 effector in regulating synaptic vesicle fusion. *Nature.* 388: 593–598.
Watanabe, K., H. Yamada, and Y. Yamaguchi. 1995. K-glypican: a novel GPI-anchored heparan sulfate proteoglycan that is highly enriched in developing brain and kidney. *J. Cell Biol.* 130:1207–1218.
Wyszynski, M., V. Kharazia, R. Shanghvi, A. Rao, A.H. Biggs, A.M. Craig, R. Weinberg, and M. Sheng. 1998. Differential regional expression and ultrastructural localization of α-actinin-2, a putative NMDA receptor-anchoring protein, in rat brain. *J. Neurosci.* 18:1383–1392.
Wyszynski, M., J.G. Valtschanoff, S. Naisbitt, A.W. Dunah, E. Kim, D.G. Standaert, R. Weinberg, and M. Sheng. 1999. Association of AMPA receptors with a subset of glutamate receptor-interacting protein in vivo. *J. Neurosci.* 19:6528–6537.
Woods, A., and J.R. Couchman. 1994. Syndecan-4 heparan sulfate proteoglycan is a selectively enriched and widespread focal adhesion component. *Mol. Biol. Cell.* 5:183–192.